OPTIMIZATION OF WELDING PARAMETERS IN COLD METAL TRANSFER WELDING OF STAINLESS STEELS

A THESIS

SUBMITTED IN PARTIAL FULFILLMENT OF THE REQUIREMENTS

FOR THE AWARD OF THE DEGREE

OF

MASTER OF TECHNOLOGY

IN

PRODUCTION ENGINEERING

Submitted By:

PRASANNA GUPTA

2K18/PIE/18

Under the supervision of

Dr. N. YUVARAJ

Assistant Professor

DEPARTMENT OF MECHANICAL PRODUCTION & INDUSTRIAL AND AUTOMOBILE ENGINEERING, DELHI TECHNOLOGICAL UNIVERSITY,

DELHI TECHNOLOGICAL UNIVERSITY

(Formerly Delhi College of Engineering)

Bawana Road, Delhi-110042

AUGUST, 2020

DELHI TECHNOLOGICAL UNIVERSITY

(Formerly Delhi College of Engineering)

Bawana Road, Delhi-110042

CANDIDATE'S DECLARATION

I, **PRSANNA GUPTA**, Roll No. **2K18/PIE/18** student of M. Tech (Production Engineering), hereby declare that the Project Dissertation titled **"OPTIMIZATION OF WELDING PARAMETERS IN COLD METAL TRANSFER WELDING OF STAINLESS STEELS"** which is submitted by me to the Department of Mechanical Production & Industrial and Automobile Engineering, Delhi Technological University, Delhi in partial fulfillment of the requirement for the award of the degree of Master of Technology, is original and not copied from any source without proper citation. This work has not previously formed the basis for the award of any Degree, Diploma Associate ship, Fellowship or other similar title of recognition.

Place: Delhi **PRASANNA GUPTA**

Date: **2K18/PIE/18**

DEPARTMENT OF MECHANICAL PRODUCTION & INDUSTRIAL AND AUTOMOBILE ENGINEERING

DELHI TECHNOLOGICAL UNIVERSITY

(Formerly Delhi College of Engineering)

Bawana Road, Delhi-110042

CERTIFICATE

I hereby certify that the Project Dissertation titled **"OPTIMIZATION OF WELDING PARAMETERS IN COLD METAL TRANSFER WELDING OF STAINLESS STEELS"** which is submitted by **PRASANNA GUPTA, 2K18/PIE/18**, Department of Mechanical Production & Industrial and Automobile Engineering, Delhi Technological University, Delhi in partial fulfillment of the requirement for the award of the degree of Master of Technology, is a record of the project work carried out by the student under my supervision. To the best of my knowledge this work has not been submitted in part or full for any Degree or Diploma to this University or elsewhere.

Place: Delhi **Dr. N YUVARAJ**

Date: **SUPERVISOR**

ACKNOWLEDGEMENT

It is a matter of great pleasure for me to present my dissertation report on "**OPTIMIZATION OF WELDING PARAMETERS IN COLD METAL TRANSFER WELDING OF STAINLESS STEELS"**. First and foremost, I am profoundly grateful to my guide **Dr. N. YUVARAJ,** Assistant Professor, Mechanical Engineering Department for his expert guidance and continuous encouragement during all stages of thesis. I feel lucky to get an opportunity to work with him. Not only understanding the subject, but also interpreting the results drawn thereon from the graphs was very thought provoking. I am thankful to the kindness and generosity shown by him towards me, as it helped me morally to complete the project before actually starting it.

I would like to extend my gratitude to **Prof. VIPIN,** Head, Mechanical Engineering Department for providing this opportunity to carry out the present thesis work.

Finally, and most importantly, I would like to thank my family members for their help, encouragement and prayers through all these months. I dedicate my work to them.

Date: PRASANNA GUPTA

Place 2K18/PIE/18

Department of Mechanical Engineering

Delhi Technological University, Delhi

ABSTRACT

For better efficiency, manufacturers these days are more interested in using very light weight materials that not only reduces the overall weight of the structure but also enables the use of latest technology. Due to their immense strength, ease in fabrication, Austenitic Stainless Steel grades find their application in wide range of manufacturing industries such as automotive, medical, construction, aerospace. Various problems such as burn through, distortions, spatter and other defects were reported when thin austenitic stainless sheets were welded using conventional arc welding process because of their high heat input. Cold Metal transfer welding is a modern era welding technology for joining of thin sheets as optimum penetration at low heat input and spatter free weld can be obtained. In this research work SS202 samples of thickness 1.58mm have been welded using SS308 filler wire by CMT welding process. Three different levels of Current (80A, 100A, 120A), Welding speed (3mm/sec, 4mm/sec, 5mm/sec), and Pulse dynamic correction Factor (-10, 0, +10) were set as input process parameter. The experiments have been carried out at most optimum parametric combination obtained from Taguchi L9 design of experiment array. The superiority of weld was estimated in the form of three mechanical properties Yield Strength (YS), Ultimate Tensile Strength (UTS), and Percentage Elongation wherein highest value obtained for the three were 379 MPa, 871 MPa, and 65.9% respectively. The experimental data obtained have been optimized by Taguchi's S/N ratio larger the better criteria. Further, Ultrasonic Assisted CMT Welding have been carried out on same SS202 samples of 1.58mm thickness under same process parameter and result have been compared with responses obtained for CMT welded samples without Ultrasonic vibrations.

KEYWORDS: CMT, Yield Strength, Ultimate Tensile Strength, Percentage Elongation, Pulse dynamic Correction Factor, Taguchi, Ultrasonic Assisted CMT

CONTENTS

LIST OF FIGURES

LIST OF TABLES

CHAPTER 1 INTRODUCTION

For better efficiency, manufacturers these days are more interested in using very light weight materials that not only reduces the overall weight of the structure but also enables the use of latest technology.

Austenitic stainless sheets of grade 200 series and 300 series are used extensively in manufacturing industries because of their excessive value of strength, resistance to temperature, ease of fabrication [Baddoo et al. (2008)] HSLA steels find their extensive utilization in ship building, and has several other industrial applications because of its favorable mechanical properties and excellent weldability [Cao et al. (2011) and Czyryca et al. (1990)] Addition of molybdenum and its low carbon content composition makes AISI 316L most suitable material to be used in manufacturing of furnace parts, exhaust manifold, jet engine and heat exchanger as it is having corrosion resistant property [Ghosh et al (2018)]. Almost all the austenitic stainless grades are welded by the GMAW process but during the welding of austenitic stainless thin sheets by conventional arc welding process high heat input causes distortions and burn through. [Reisgen et al (2019)].

Magnesium alloys are most promising materials of the latest era due to its high strength and stiffness. But because of its hexagonal closed packed structure which is having improper slip systems at room temperature, manufacturing of complex shapes and parts is very expensive. [Coelho et al. (2008)]. To solve the joining problem of magnesium alloys many welding process have been used such as gas metal arc welding (GMAW), friction stir welding (FSW), electron beam welding (EBW) and others. Among all these welding processes GMAW has given very efficient results. [Min et al. (2009)]. There are so many problems that has been reported during fusion welding of Mg alloys and Al alloys. Since Magnesium are one of the lightest material which are used in automobile and aerospace industries they have potential to form hybrid structure with aluminum alloys which can reduce the weight of the overall structure. [Zeng et al. (2001)]. Weld bead of magnesium alloy is very likely to have coarse grain in addition to this there is high probability of evaporation, oxidation, and hot cracking during the welding. Hence, there is immense need to use a welding technology by which a stable and controlled heat input can be given. [Feng et al. (2005)]

Aluminum provides high resistance to corrosion as well as high strength to weight ratio and their addition with steel, is considered as most promising in manufacturing industries. During early era, welding of aluminum alloys was very limited as less strength and more heat affected zone (HAZ) was obtained using the conventional welding process. Although, Tungsten Inert Gas (TIG) and Metal Inert Gas (MIG) welding were invented and most of the industries used these processes for welding of aluminum but still low joint efficiency and numerous defects in welded joints were reported due to high heat input rate. [Gungor et al (2014)]

As pollution is increasing day by day there is immense need to take measures to reduce pollution and save our energy sources. It is highly appreciable if hybrid structure is used where steel and aluminum can be joined to make automobile parts lighter. [Cole et al. (1995)] Joining of these dissimilar metal by fusion welding has always been an issue because of the formation of the intermetallic compounds**.**

Traditionally all these materials were welded by using arc welding method like MIG/MAG welding, TIG welding. Shielded Metal arc welding (SMAW) provides higher heat input which results in the formation of the coarser grains and wider heat affected zone. [Nathan et al. (2005)]. Welding of thin sheets of these materials is very difficult at constant high heat energy that is given in these conventional process. During the welding process temperature variation in the parent metals and the welds shows effect on heat affected zone, dimensional accuracy, residual stresses and microstructure characteristics of the weld [KURSUN et al. (2008)]. There was immense need to develop the technology which gives optimum heat as input for welding of these materials.

[Koli et al. (2020)] reported that for same current CMT showed low amount of bead penetration when evaluated against MIG Pulse and MIG manual, hence thin sheets can be welded by using CMT. [Frostevar et al. (2014)] reported that CMT arc mode showed better weld bead stability, less under cut, less heat affected zone and required less power as compared to pulsed and standard arc mode. [Stanciu et al. (2017)] reported that by reducing wire feed rate reinforcement in CMT welding can be reduced whereas increasing the welding speed results in improper penetration. Defect free and porosity less weld overlay of Inconel

617M over SS316 sheets can be obtained by Cold Metal Transfer Welding Process. [Varghese (2019)].

An optimum penetration of the weld bead with high dilution and a huge depletion in residual stresses value was discovered by [Koli et al. (2020)] using CMT joining technology. CMT arc mode was reported to have least welding defects with negligible distortions along with best mechanical properties were obtained in comparison to standard and pulsed mode. [Lei et al. (2017)]. Less heat affected zone was reported for CMT as compared to MIG and GTAW. [Dharmik, et al. (2020)]. The best mechanical properties were obtained using CMT arc mode in comparison to standard and pulsed mode. Under the CMT arc mode, welding with chill block under the bottom sheet could prevent the downfall of the weld metal and the accelerated heat dissipation which results in the negligible heat affected zone. [Lei et al. (2017)].

1.1 COLD METAL TRANSFER WELDING PROCESS

Cold Metal Transfer Welding is a latest technology which is modification to MIG welding. In this superior welding technology, the filler wire is drawn backward and forward which is an alternative to continuous wire feed with the aid of a creative wire feed system which is coupled with control system [Selvi et al. (2018)]. The detachment of droplet during short-circuit is assisted by this wire retraction motion hence, the droplet is fetched into the weld pool without any help of the electromagnetic force [Schierl et al. (2005)]. Using CMT welding process accurate material deposition rates are obtained and current parameters are controlled very precisely, this helps in giving low thermal energy which is ample and adequate to liquefy both filler wire and base material hence, less distorted spatter free weld bead is obtained [Zhang et al. (2012)]. The above quoted advantages of CMT welding technology makes it suitable process for joining various similar and dissimilar metal [Chen et al. (2017)]. The whole droplet transfer cycle or process is carried out three phases as shown in figure 1.1

[a] The peak current phase: In the peak current phase high pulse of current is there along with constant arc voltage. This high pulse of current ignites the welding arc easily and then forms the droplet by heating the wire electrode.

[b] The background current phase: The background current phase corresponds to lower current. Since a little liquid droplet is formed on the wire tip in the peak current phase so in order to inhibit the globular transfer the current is dropped very drastically in the background phase and the constant low level of current is kept until the short circuiting process happens.

[c] The short-circuiting phase: In the short-circuiting phase, weld pools contacts with the wire, with arc voltage dropping to zero arc is extinguished. The back-drawing force is the main factor that urges the droplet to break away from the wire into the weld pool. In this phase the liquid fracture and transfer of material into the welding pool finally takes place. [Kursun et al. (2008]

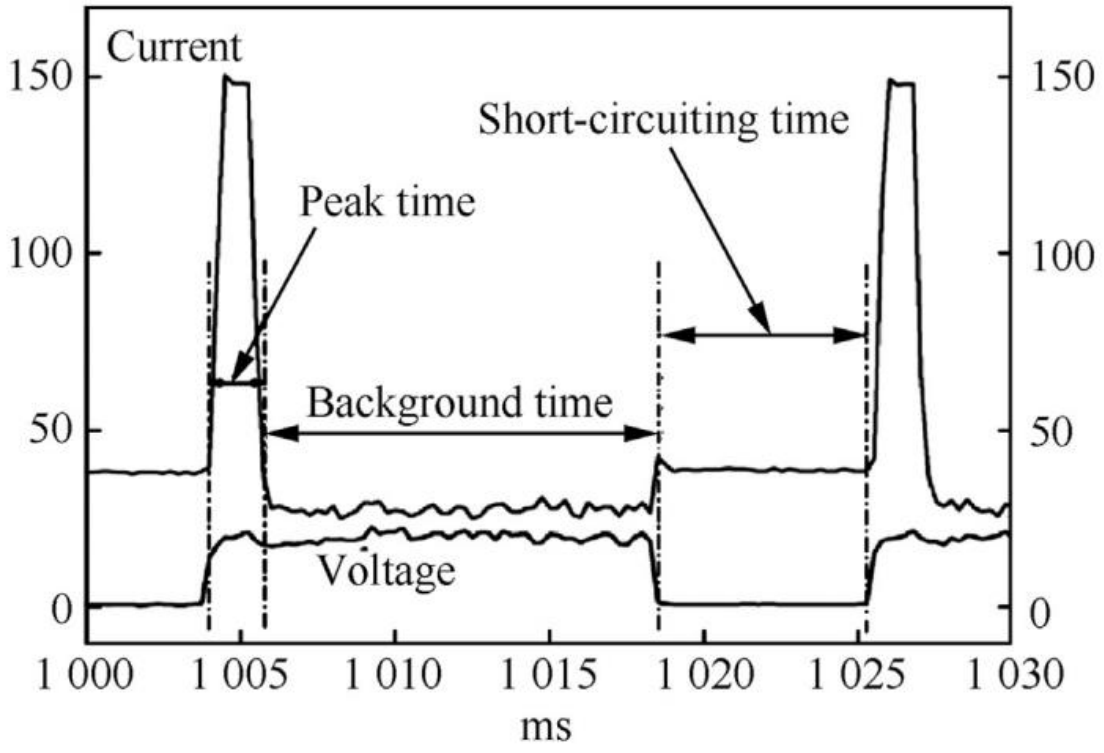

Figure 1.1: The current and Voltage Waveforms of the CMT process [Selvi et al. (2018)]

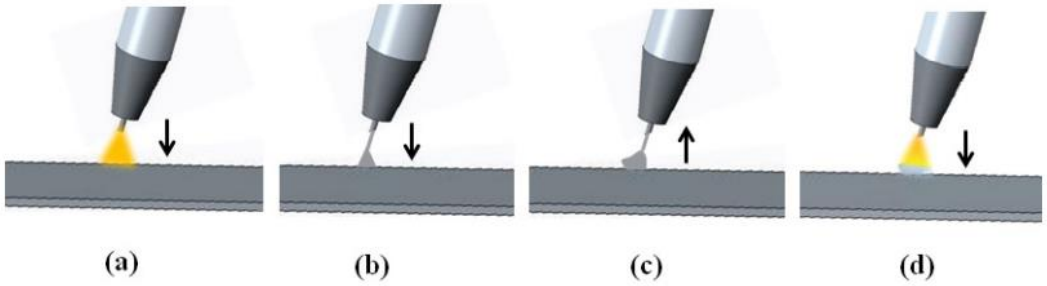

Figure 1.2: CMT welding process – Different phases of wire feed motion [Sravanthi et al. (2019)]

Figure 1.2 represents the how the wire feed motion occurs in different phases in CMT welding process. The whole process is explained in the form of figure (a), (b), (c) and (d) as discussed below:

a) The wire feed motion towards the weld pool during arcing period
b) As the wire is dipped into the molten weld pool, process of short circuiting takes place due to which arc is extinguished and the value of welding current comes to lower value.
c) The moment at which retraction of the wire takes place, the backward or rearward movement of wire serves the purpose of detachment of the droplet during the short circuit.
d) Since the transfer of metal is also assisted by the Surface Tension, this results in controlling the value of current to a very low value which results in overall reduction in input of heat and hence spatter is reduced. In this the wire is reversed and the process starts from the beginning again. In this manner the process is continued again and again. [Sravanthi et al. (2019) and [Kursun et al. (2008]

Current of zero magnitude is there during short circuiting which is 25% of total time during CMT welding. This reduces the energy consumption to 30 to 40 percent and hence the cost incurred is also reduced. [Kumar et al. (2018)]. The tensile strength obtained by CMT welding process was very close to the tensile strength obtained by Friction Stir welding. Also, the yield strength obtained by CMT welding process was reported to be higher than obtained by any other welding processes such as MIG welding process, Friction Stir Welding process that too at very low heat input. CMT welding process required low heat input as compared to conventional MIG welding process and almost negligible distortion of the welded plate

was obtained. [Gungor et al. (2014)]. CMT welding process reduces the thickness of the brittle intermetallic layer which is formed at the interface of aluminum and steel welded joint. [Zhang et al. (2008)]. Porosity was drastically reduced in the weld bead of AA2219 aluminum alloy samples when welded by CMT welding in comparison to conventional welding processes. [Cong et al (2016)]

1.2 STAINLESS STEEL

The main constituent in the stainless steels is iron. The other main element that must be present in the material is chromium which should at least 10.5 % than only the given material be considered in the stainless steel category. These are the corrosion resistant steels because of high chromium content. The rapid oxidation is prevented due to formation of protective oxide layer due to reaction of oxygen with chromium and hence corrosion is resisted. The other elements such as Nickel, Molybdenum, Carbon, Manganese, Silicon, Sulphur, Carbon, Niobium Titanium, Copper and Nitrogen is added in varying quantity to obtain the different grades of Stainless steels. [Jurica et al. (2018)].

Stainless steels find their application in different fields such as automobile industry, fabrication of sheet metal, chemical industry, manufacturing of railway coaches Cooking utensils, Railway equipments, Motor shafts of boats Petrochemical Industries Power and Transportation, Paper and oil industries [Devakumar et al. (2014), Ra Sudhakaran et al (2014), Vignesh et al. (2015) and Jurica et al. (2018)].

1.2.1 TYPES OF STAINLESS STEEL

Different types of stainless steel as per ASM standard is as follows:

1) Austenitic Stainless Steel: These cover the major portion of stainless steels in terms of different types of alloys and usage. There are further subdivide into two categories:

a) AISI 300 series: These are mainly iron, chromium, nickel based alloys. Such as SS301, SS302, SS304, SS308, SS316. The range of chromium is in between 16% to 26%, for

nickel range is in between 10% to 22% and also contains Titanium, Molybdenum, Niobium and Nitrogen.

b) AISI 200 series: These are mainly iron, chromium, nickel and manganese based alloy. In this molybdenum range is in between (5% to 18%) which replaces the nickel. As nitrogen is added in this they show higher yield strength than that of 300 series.

Austenitic Stainless steel grades possess high ductility, excellent resistance against corrosion and other functional characteristics that makes it suitable material for usage in manufacturing industries. [Kujanpaa et al. (2014) and Lyon et al. (2015)] In addition to this they show excellent toughness and resistance to temperature. [Ishimaru et al. (2014)]. They can be made soft easily and are easily deformable, and also they can become also become extremely hard by cold working. This means yield strength can vary between 200 MPa to 2000 MPa for stainless steel. Even in softer condition Tensile strength of austenitic Stainless steel is greater than that of mild steel. In softer condition stainless steels possess exceptional ductility and high value of percentage elongation of about 50%. Further the stainless steel can undergo the process of cold working and hence, can be used for the manufacturing of several goods and products. [Jurica et al. (2018)]. They show excellent weldability and formability. These are essentially nonmagnetic. Addition of Sulphur, Phosphorous and manganese also improves the weldablity [Reisgen et al. (2019)]

2. Ferritic Stainless Steels: These contains Iron and chromium as their major composition. These are 400 series alloys containing chromium in the range of 11 % to 27% and with an addition of small amount of stabilizers such as Aluminum, Niobium, Titanium that stabilizes the ferrite. These material do not get hardened. Recent development showed the evolution of Super ferritics material having chromium up to 30% with 4% molybdenum and 2% nickel. They are resistant to SCC (Stress corrosion cracking). They do not possess good weldability and problem of grain growth is there. Because of these problems in welding very thin thickness sheets are not used for the construction of large structures.

3. Martensitic Stainless Steel: These possess many properties and are resistant to creep. The chromium content is in the range of 12 % to 15% in addition to this 0.2 to 1% molybdenum is also present. The amount of Carbon content is 0.1% to 1% and amount of nickel present

is nil. Presence of these element makes them ferromagnetic. They show wear resistant properties with high resistance to corrosion and excellent toughness. They are used in aerospace industries.

4) Duplex Stainless Steel: The ratio of Ferrite and Austenite is maintained to 50% each so that desirable mechanical properties can be achieved. They are having chromium in the range of 19% to 32% and molybdenum up to 5 %. Theses possess a larger value of toughness and supreme weldability in comparison to ferritic stainless steel [Chan et al. (2014)]. These also possess formability and weldability up to a certain extent.

5) Precipitation hardening stainless steel: They use about 17 % chromium and 4% nickel content having comparable strength to austenitic stainless steel and can be hardened to further improve the strength.

1.2.2 PROPERTIES OF SS 202 MATERIAL

Austenitic steel grade such as SS202 which is having high chromium and manganese content as shown in Table 1.1 is less expensive material as compared to other grades having comparable strength and shows excellent toughness and stability at room temperature. Yield Strength of SS202 increases because of addition of manganese [Vignesh et al. (2019)]. Higher strength to weight ratio is reported for SS202 amongst other austenitic stainless steel grades [Kumar et al. (1996)]. Higher limiting draw ratio is reported for SS202 as compared to SS304 austenitic stainless steel grades [Du Toit et al. (2012)]. Table 1.2 shows the mechanical properties of SS 202 material.

Table 1.1. Chemical composition (% wt) of grade 202 stainless steel [Pradhan et al (2019)]

Fe	Cr	Mn	Ni	Si	N	C	P	S
68%	17-19%	7.5-10%	4-6%	≤ 1%	≤ 0.25%	≤0.15%	≤0.060%	≤0.030%

Table 1.2. Mechanical properties of grade 202 stainless steel [Pradhan et al (2019)]

Properties	Value
Tensile Strength	515 MPa
Yield Strength	275 MPa
Elastic Modulus	207 GPa
Poisson's Ratio	0.27 to 0.30

These properties make SS202 suitable material to be used in the following applications: [Vignesh et al. (2015) and Ra Sudhakaran et al (2014)].

a) Plates or sheets in the manufacturing of cooking utensils,

b) Motor shafts of boats,

c) Railway components,

d) Medical devices,

e) Restaurant equipment,

f) Automotive trim,

g) House sink

1.3 PROCESS PARAMETERS

1) Current: Heat input is directly proportion to current value. [Dhobale et al. (2015)]. Current value influences the microstructural and mechanical properties and also the depth of penetration. Too high or too low current results in inadequate penetration of the weld. The value of current should be chosen on the basis of thickness of the base material. Too high current can also cause burn through. In this research work current is chosen as the independent process parameter and three independent value are set.

2) Voltage: Arc voltage is also directly proportional to the heat input. [Dhobale et al. (2015)]. In this study Current is chosen as independent process parameter and value of Voltage is dependent on the current. Changing the current value automatically changes the value of voltage. A constant voltage is maintained throughout the process

3) Welding speed: Welding speed is inversely proportional to the heat input. [Dhobale et al. (2015)] such that increase in welding speed results in low heat input and may result in improper penetration on the other too low welding speed can result in the high heat input which may cause the burn through. The welding speed is simply the ratio of total distance travelled by welding torch over the plate to that of total time taken by the welding torch to complete that distance. In this research work welding speed is chosen as the independent process parameter and three independent value are set.
4) Pulse Dynamic Correction factor: This parameter is provided in the CMT welding machine to slow down or accelerate the droplet detachment at a constant energy level. The pulse dynamic correction factor controls the average current and influences the direct current [Rajeev et al. (2019)] For correcting the pulsing energy of a pulsed arc Pulse dynamic correction factor can be set at 3 different levels, that are -10, 0, and +10 wherein -10 represents that detachment force for the droplet is on lower side, 0 represents that there is no increase of decrease in the droplet detachment force and +10 represents that force for detaching the droplet is on the higher side. In this research work Pulse dynamic correction factor is chosen as the independent process parameter three independent value are set.
5) Gas flow rate: This parameter defines the flow rate of the shielding gas. Gas flow rate affects the quality and microstructure of weld bead. Shielding gas shields the molten weld pool from harmful atmospheric gases. In this research work a constant value of gas flow rate was maintained.
6) Contact Tip to work distance: The distance between the filler wire tip to the base metal is the contact tip to work distance or CTWD. An optimum value of CTWD should be maintained. Decrease or increase in the CTWD values directly influence the current value. In this research work constant value of CTWD is set for all the experiments.
7) Wire feed rate: Wire feed rate directly influence the HAZ, weld width heat input and thickness of intermetallic layer. [Milani, et al. (2016)]. It is defined as the rate at which filler wire is feed towards the weld bead.

CHAPTER 2 LITERATURE REVIEW

2.1 CMT WELDING OF SIMILAR METALS

2.1.1 CMT WELDING OF STEELS WITH SIMILAR MATERIALS

[Kadoi et al. (2016)] investigated use of cold metal transfer welding in crack repairing of long term used steam turbine cases of Cr-Mo-V cast steels. The experimental result concluded that CMT welding using low melting point filler wire BAg-8 is suitable for crack repairing of turbine cases. The process is very sustainable as it prevents the formation of the hardened phases in heat affected zone and creates a very wide weld bead.

[Chen et al. (2017)] investigated effect of current waveform on welding of mild steel sample using cold metal transfer welding. Q235 mild steel samples of thickness 3 mm was welded using ER50-6 filler wire of diameter 1.2mm and pure CO_2 of gas flow rate 15 L/min as shielding gas. The experimental result reported that at wire feed rate of 5 m/min increasing the current from 250A to 320A did not affect the stability of the weld. The average wire feed rate, rate of deposition and the size of droplet was increased with increase in the boost current although the average wire feed rate was kept as constant. Increasing the boost current also increases the weld bead width and the penetration.

[Bunaziv et al. (2018)] investigated the weld bead properties of high strength low alloy steel welded by hybrid laser arc welding in cold metal transfer welding mode by preplacing the wire in the weld groove prior to welding. The test result concluded that preplacement of the wire in the weld groove significantly improved the stability and homogeneity of the weld. It was had shown some disadvantages as well as it is less attractive economically and also limited to flat welding only in horizontal direction.

[Reisgen et al. (2019)] investigated mechanical and microstructure properties of the weld bead of austenitic stainless steel AISI 304 samples of thickness 3 mm welded by cold metal transfer welding process using ER 308LSi filler wire of diameter 0.8 and 1.2mm. For shielding gas mixture of argon and carbon dioxide was used. With Ar as 97.5% and CO_2 as 2.5%. The test result concluded that all the sample undergone ductile fracture. The hardness

of the weld bead obtained was in the range of 200-250 HV with base metal having nearly same hardness value.

[Lei et al. (2019)] welded S355J2W+N steel of thickness 6 mm using hybrid laser- cold metal transfer welding process and evaluated the behavior of droplet transfer. The filler wire of NiCu 1-IG of diameter 1.2 mm was used. The experimental result concluded that most influential parameter for the droplet transfer frequency in CMT process is the welding current. Because of the thermal effect the droplet size was increased and wire tip melted very fast so as to slow down the droplet transfer frequency. In high speed welding condition the laser can stabilize the arc and avoid the effect of wire adhesion. Further the experimental result concluded that transfer frequency and formation of weld was improved by laser.

[Yu et al. (2017)] welded zinc coated steel of thickness 2.3mm using 1.2 mm diameter metal core welding filler wire. The effect of composition (such as C, Si, Mn) of filler wire on the weld porosity formation was evaluated in the experimental part. The experimental results concluded that the presence of Si and Mn contents effectively reduce the weld porosity. On reducing the Si and Mn contents viscosity of the weld pool also decreased with an increase in the emission of zinc vapor which impacted the hardness of the weld. On decreasing the Mn content of the filler wire resulted in the decrease in the electrical resistance of the wire. The best composition for the metal cored wire was found to be (0.51% Mn content, 0.3 % Si content and 0.08% C content) which very effectively reduced the porosity of the weld. The wire was classified as ET70T15-M20AZ-G.

[Alipooramirabad et al. (2017)] investigated the effect of welding process on residual stress of the weld bead formed while welding high speed low alloy steel of thickness 20 mm using E6010 electrode of diameter 3.2 mm and E8010 electrode of diameter 4mm. The experiments were carried out in three modes which are shielded metal arc welding (SMAW), modified short arc welding (MSAW) and flux cored arc welding (FCAW). The experimental result concluded that in SMAW mode the heat affected zone increased due to which the residual stresses were found to be further away from the weld bead. Residual stresses of significant level were reported when arc mode was changed to MSAW and FCAW.

2.1.2 CMT WELDING OF ALUMINIUM WITH SIMILAR MATERIAL

Recently, the development of Cold Metal Transfer welding technology is considered as the major achievement for welding of aluminum specimen. [Kumar et al. (2016)] investigated the weld bead characteristics of AA6061 aluminum alloy welded by Cold Metal Transfer Welding process using filler wire of same composition as of base metal which resulted in quasi binary weld bead which is less prone to hot cracking, and gives less heat affected zone. The microstructure test result also discloses that fine recrystallization was obtained at the joints with uniform distribution of grains at the base metal and at the heat affected zone which were visible clearly due to difference in their sizes.

CMT welding of AA6061 aluminum alloy specimen of thickness 2mm at different polarity was carried out by [Guojin et al. (2018)] using ER 4043 filler wire of diameter of 1.2 mm. The experiments were carried out at 7 mm/sec welding speed and 7 m/min fire feed rate. The test result data concluded that micro hardness value that was obtained was in the range between 52 to 77 HV which decreases at heat affected zone. The fracture mode of joint was ductile fracture and porosities were found to be very less. The fracture was reported to occur at the HAZ.

[Rahul et al. (2018)] investigated the influence of CMT welding process on depth and width of penetration of weld bead of AA6061 aluminum alloy sample of thickness 2mm at constant gas flow rate of 18 l/min. The test result concluded that initially the welding current increases to a value of 50A and as the short circuit occurs the welding current reduces because of inability of conventional controller to retain the current. But on the other hand the controller that is available with CMT welding machine retains the current at 50 A as it detects the short circuit which results in uniform depth of penetration of weld bead.

[Elrefaey, et al. (2015)] investigated the properties of weld bead of AA7075 aluminum alloy which is welded by CMT welding process. The test result data discloses that very low porosity, spatter free joints were produced. The joints also reported to have minimum micro hardness in weld zone which further decreases in Heat affected zone. The coefficient of ultimate tensile strength, yield strength and elongation was found to be 60%, 77% and 69% respectively which was better when compared with conventional MIG welding and TIG

welding and of comparable magnitude when compared with Laser beam welding and Friction stir welding.

[Dutra et al. (2015)] investigated the effect of Cod Metal Transfer Welding Process on weld bead of AA5083-H116 aluminum alloy welded by using Al 5183 and Al 5087 filler wire. Better tensile strength was obtained when welded by using Al 5087 filler wire. The micro hardness was reported to be similar in both Heat affected zone and welding zone. Also, both the wires showed same toughness. Toughness results also indicated good crack resistant properties.

2. 2 CMT WELDING OF DISSIMILAR MATERIAL

2.2.1 CMT WELDING OF STEEL AND ALUMINUM

Investigation of arc length characteristics and behavior of metal transfer was done by [Zhang et al. (2009)] while welding of hot dip galvanized steel samples with pure aluminum 1060 samples of thickness 0.6 mm and 1 mm respectively. Based on the experimental data it was concluded that the transfer of metal using CMT process was found to be very steady. The heating behavior of arc is based on the features related to wave control. The lap joint was reported to be crack free between dissimilar steel and aluminum samples and the joint contains intermetallic layer of $FeAl_3$ and Fe_2Al_5.

[Mezrag et al. (2020)] investigated microstructure properties of weld bead formed between 6061-T4 aluminum alloy and zinc coated DC01 mild carbon steel samples of thickness 1mm using ER4043 filler wire of diameter 1.2 mm diameter using cold metal transfer welding process. The experimental data reported that because of dissolution of hydrogen in liquid aluminum dispersed porosities were reported in upper part of the weld and because of vaporization of zinc coating larger porosities were reported in the weld root and size of these porosities were reported to increase as the welding power is increased. The failure of lap joint formed between the two was reported to get initiated in the weld root symmetrically which further propagates along the interface of the weld bead. Further it was reported that shear strength of the weld bead reaches to three-fourth base plate of aluminum when the power is

low and welding speed is high but to excessive increase in the weld bead result in large porosities with reduce the strength.

[Cao et al. (2014)] investigated weld bead properties of the joints formed between galvanized steel Q235 and aluminum alloy AA6061-T6 samples of 1 mm thickness using ER4043 filler wire and 100% argon as shielding gas using cold metal transfer process. The investigation results disclosed that if fire wire feed rate is controlled than satisfactory results were obtained and the most optimized wire feed rate that was reported was in the range of 7.5 m/min to 8 m/min.

[Sravanthi et al. (2019)] evaluated the corrosion behavior of weld bead formed between aluminum alloy and galvanized mild steel sample welded using cold metal transfer process. Lap joints were formed between H32 5052 aluminum alloy and galvanized mild steel of thickness 3 mm using Al-Si filler wire at different process parameters. The test result concluded that the presence of Al-Fe and Al-Fe-Si phases in the intermetallic layer are the main reason for the worsening of corrosion resistance of the weld bead. When these CMT welded samples are exposed to nitric acid the IMC layer found was reported to get dissolve completely within 24 hours. The weight loss due to corrosion was found to be very less in CMT welded samples as compared to GMAW-braze weld.

[Singh et al. (2020)] evaluated the properties of weld bead formed between AA5052 aluminum alloy and DP780 steel samples using cold metal transfer welding process. The different experiments were conducted while varying the thickness of aluminum samples and lap joint was formed between the samples. From the experimental results it was concluded that as the thickness of aluminum samples increased the wettability was decreased because fluidity of molten filler decreased on the steel surface. This is due to the higher rate of dissipation of heat from the molten pool which also reduced capacity of bearing load of the lap joints formed. Further it was reported that brittle and hard Al-Fe-Si ternary phases are formed at the interface of steel and bead deposit. Thickness of intermetallic layer was increased as the heat input was increase. Increase in wire feed rate increases the wettability of the joints. Furthermore, the experimental result showed that increase in wire feed rate failure load initially increased, reaches the maximum value and then started to decrease despite increase in wettability because the thickness of intermetallic layer also increased.

[Cao et al. (2014)] welded AA6061-T6 aluminum alloy with boron steel samples using cold metal transfer welding. The aluminum alloy sample of thickness 1 mm and boron steel sample of thickness 1.5 mm were taken and welded using Al4043 filler wire of diameter 1.2mm. The experimental results reported that zinc was evaporated from galvanized boron steel and the heat dissipation from the evaporation of zinc reduced the temperature of the zinc. Further it was reported that bare boron coated and Al-Si coated boron steel joints with aluminum alloy AA6061-T6 sample could not be formed because of the formation of large brittle intermetallic layer formation.

2.3 CMT WIRE ARC ADDITIVE MANUFACTURING PROCESS

Wire arc additive manufacturing is a three dimensional rapid prototyping process based on cold metal transfer welding process in which final shape of the component is obtained through layer by layer deposition of fused wire. It is reported that parts manufactured by CMT WAAM are of high quality and very much economical.

[Caballero et al (2019)] investigated the effect of variation of different process parameters such as deposition rates and gas flow rate for producing specimens by wire arc additive manufacturing process. The specimens were prepared using precipitation hardened stainless steel filler wire of diameter 1.2 mm diameter. After the preparation of all the specimen different tests were conducted such as tensile test, residual test and Vickers hardness test. In addition to these test microstructure images of the samples was also examined using electron microscope. It was reported that desired tensile strength can be obtained using the above process after the appropriated heat treatment process post deposition. Further the test result discloses that the direct ageing resulted in formation of harmful intermetallic phases which leads to the embrittlement of the deposit and retained austenite formation is directly dependent on the rate of cooling.

[Dirisu et al. (2019)] investigated fracture toughness of CMT- WAAM deposited steel samples. The gas flow rate in the experiment was kept to 15L/min, shielding gas (Ar-80% + 20% CO_2) for 1.2mm diameter ER70S-6 and ER120S-G filler wire and (Ar-2%O_2) for same diameter ER90S-B3 filler wire was used. S275 JR plate of thickness 15mm was used as the

base plate in the experiment. The experimental result concluded that the variation the fracture toughness was due variation of softening and hardening which is dependent on the cooling rates and variation of peak temperature. The fracture toughness across the direction of deposit reported most resistance to the fracture failure because of reduction in grain size. The fracture toughness was reported to show least resistance to fracture failure in the welding direction because of the increased grain size. The fracture reported was ductile fracture.

[Ge at al. (2018)] investigated microstructure and mechanical properties of 2Cr13 thin wall part deposited by wire arc additive manufacturing using cold metal transfer welding process. The sample size obtained was 150 mm ×150 mm ×8 mm. The residual stress in next layer can be reduced by preheating the previous layer. The cooling rate first decreased very quickly because of direct chilling effect but after that it remained stable from 15-25th layer due to similar conditions. The amount of martensite was reported to increase gradually from 5th layer to 25th layer which suggest that martensite decomposed into the ferrite because of diffusion of carbon with supply of thermal energy. The hardness was reported to be very less in the middle and bottom layer which increased quickly in the 20 to 25th layer with decrease in ductility. The fracture process changed from ductile in the 1st to 10th layer to in between ductile and brittle in 15th to 20th layer and finally to brittle in the topmost layer.

Table 2.1 and 2.2 discusses the literature survey based on the published work in the field of CMT welding of steels with various similar and dissimilar materials based on the different process parameter. Table 2.3 specifically shows the published work for welding Austenitic stainless steels.

2.4 LITERATURE REVIEW BASED ON PROCESS PARAMETER

Table 2.1. Literature Review of Published work on CMT welding of steel with similar Metals

S. No.	Author and Year	Material Used	Filler Wire Used	Process Parameter	Results and Conclusion
1.	Li et al. (2014)	Q235 Mild Steel Plate	ER70S-6 Filler wire of dimeter 1.2 mm	Thickness of plates – 10 mm Gas flow rate – 20L/min Speed – 1 m/min Wire feed rate – 9 m/min The experiments were carried out in different arc mode i.e. CMT, Standard and Pulsed. For CMT arc mode Current – 198 A Voltage – 14.9 V For Standard arc mode Current – 204 A	(1) The experimental results reported that CMT arc mode was most stable and resulted in least spatter while Standard arc mode resulted in highest spatter. (2) It was further observed that CMT mode resulted in smallest mean grain size while Standard mode was having the largest. (3) The Ultimate tensile strength results showed that the strength decreases from CMT arc mode to Pulsed arc mode and least strength was reported in Standard arc mode.

				Voltage – 22.8 V For Pulsed arc mode Current – 235 A Voltage 23.8 V	
2.	Frostevar et al. (2014)	S420 MCD Mild Steel Plate	ER70S-6 Filler wire of diameter 1.2 mm	Thickness of plates – 10 mm The experiments were carried out in different arc mode i.e. CMT, Standard and Pulsed. Case 1 Speed – 2m/min Wire feed rate – 4m/min For CMT arc mode Current – 132 A Voltage – 13.2 V For Pulsed arc mode Current – 102 A Voltage – 29.4 V	(1) The experimental result concluded that CMT arc mode is most suitable for thicker steel plates. (2) CMT arc mode also showed better weld bead stability, less under cut, less heat affected zone and required less power as compared to pulsed and standard arc mode. (3) Further the experimental data concluded that undercut is directly proportional to welding speed as welding speed was increased undercut also increased for wider gap. (4) In addition to this as the welding speed increases irregularities in arc behavior was reported which resulted in variation of weld bead.

				For Standard arc mode Current – 168 A Voltage – 19.2 V Case 2 Speed – 5 m/min Wire feed rate – 8 m/min For CMT arc mode Current – 228 A Voltage – 16.5 V For Pulsed arc mode Current – 195 A Voltage – 25.7 V For Standard arc mode Current – 244 A Voltage – 24.8 V	(5) CMT arc mode showed very less sensitivity to speed change.
3.	Ahsan et al. (2016)	Hot rolled Zinc Coated	ER70S-3 Solid filler wire of diameter	Thickness of sheets - 2 mm	(1) The experimental results reported that minimum heat input of 200J/mm is required to ensure minimum

		Steel	1.2mm	Current – 120 A to 263 A Voltage – 12 V to 20 V Speed – 40 cm/min to 120 cm/min Different sets of experiments were conducted with these parameters	penetration of the weld for the given material. (2) At different heat input temperature of the weld was found to be 1650°C at 250J/mm, 2100°C at 250-350J/mm and 2700°C at 350-550J/mm. (3) Further, the experimental result showed that at low heat input the zinc bubble could not grow and rise due to high viscosity of weld pool which resulted in small sized pores which were formed near weld root and less porosity was reported, On the other hand at high heat input high temperature of weld pool resulted in delayed solidification, hence zinc bubble could grow and escape viscosity of weld pool was less.
4.	Stanciu et al. (2017)	S235JR Low Carbon Steel	ER70S-6 Filler wire of diameter 1.2 mm.	Thickness of sheet – 1 mm Gas flow rate – 15L/min Current – 85 A Voltage – 18.3 V	(1) The experimental result concluded that compared with synergic pulse welding better results were obtained with CMT.

				3 samples were tested with conventional synergic MAG welding and 3 with CMT welding at 3 different speed 600mm/min, 800mm/min and 1000 mm/min	(2) By reducing wire speed reinforcement in CMT welding can be reduced. (3) Further it was reported that increasing the welding speed results in improper penetration
5.	Kannan et al. (2019)	AISI 316L Low carbon austenitic stainless steel	ER 308L Filler wire	Thickness of sheets - 2mm Current - 105A Voltage - 12.5V Speed - 350mm/min Gas flow rate – 20L/min 9 samples were tested at different arc length correction factor from -20% to +20%.	(1) The effect of single process variable that is arc length correction was tested on mechanical properties of weld bead. (2) The experimental result concluded that as the arc length correction increases the top reinforcement also increased. (3) The tensile strength of weld joint increases when arc length correction increases from 0% to 20% and the best weld bead profile was given by 10% arc length correction. (4) The maximum tensile strength, yield strength and percentage elongation were reported to be 569 MPa, 221 MPa, and 36.47%.

6.	Luchten-berg, et al. (2019)	S32205 Duplex Stainless Steel	ER2209 Filler wire of diameter 1.2 mm	Thickness of plates - 12mm Current - 215A Voltage - 20V Different experiments were conducted by varying the welding speed as 15 cm/min, 23cm/min, 30 cm/min,	(1) Different sets of experiment were conducted at different heat input which was varied by changing the welding speed. (2) The experimental results concluded that the change in heat input changes ferrite/austenite balance. As the energy increases intergranular austenite formation also increases. But the formation of ferrite decreases. (3) At higher heat input the weld overlay showed the less resistance to corrosion as compared to base steel plate as compared than at lower heat input. (4) Hardness of the weld overlay was reported to be higher than the rolled S32205 plate due to the large number of austenite/austenite and austenite/ferrite interface.
7	Dharmik, et al. (2020)	CRNGO thin electrical steel sheets	ERCuSi$_3$, ER316L, ER70S6,	Thickness of sheets – 0.5 mm	(1). The most significant effect was on the properties of the weld was shown by MIG welding and GTAW.

			3 filler wires were selected.		(2) Less heat affected zone was reported for CMT as compared to MIG and GTAW.

Table 2.2 Literature Review of Published work on CMT welding of steel with dissimilar Metal

S. No.	**Author and Year**	**Material Used**	**Filler Wire Used**	**Process Parameter**	**Results and Conclusion**
1.	Zhang et al. (2008)	1.Q235 cold rolled zinc coated low carbon steel. 2.Wrought aluminum 6061	AlSi5 alloy filler wire of diameter 1.2 mm	Thickness of sheets - 1mm Voltage – 11V to 12V Feed rate - 3.7 m/min to 3.8m/min Speed - 13.9 m/min to 14m/min Gas flow rate – 15L/min	(1) The experimental result concluded that intermetallic layer formed between zinc coated steel and wrought aluminum are mostly in $FeAl_3$ phase. (2) CMT welding has increased the strength of joint with less heat input that has also affected the thickness of brittle intermetallic layer**.**
2.	Yang et al. (2013)	1.Zinc coated low Carbon Steel	ER 4043 Filler wire of diameter 1.2mm	Thickness of steel sheets - 1.2mm Thickness of aluminum alloy sheet – 2mm	(1) The experimental result concluded that Pre-setting gap can allow zinc vapor to escape and hence stabilize the welding process.

		2.6061-T6 Aluminum Alloy		Gas flow rate - 16L/min Speed - 0.5m/min Sample were tested at different pre-set gap of 0mm, 0.1mm, 0.3mm, 0.5mm Samples were also tested at different offset distance of 0mm, 1mm, 2mm.	(2) Further, in tensile test it was reported that weld strength was directly proportional to preset gap and inversely to offset distance.
3.	Lin et al. (2013)	1.Zinc coated low Carbon Steel 2.6061-T6 Aluminum Alloy	ER 4043 Filler wire	Thickness of steel sheets - 0.7mm and 1.2 mm Thickness of Aluminum alloy sheet - 2 mm Current - 70A Voltage - 11.5V Speed – 0.7 m/min 2 sets of experiments were conducted.	(1) Shear strength of joints were tested by both numerical modelling and experimental measures. (2) High strength was reported in joint between aluminum alloy zinc coated steel with thickness 1.2 mm (3) Low strength was reported in joint between aluminum alloy zinc coated steel with thickness 0.7 mm. (4) Maximum principle stress theory and deformation energy was reported as the failure

					criteria at interface and plastic strain for failure at fusion line.
4.	Milani et al. (2016)	1.Galvani-zed Steel 2. 5754 Aluminum Alloy	$AlSi_3Mn$, $AlSi_5$, $AlSi_{12}$ 3 filler wire of diameter 1.2mm	Thickness of Galvanized Steel – 2mm, Thickness of 5754 Aluminum Alloy – 3mm, Wire feed rate – 4.7 m/min, 5 m/min, and 5.3 m/min. Welding speed – 10mm/sec Gas flow rate – 17L/min Stick out 17mm	(1) Metallurgical properties of the welded joints was changed due to addition of Silicon in filler wire. (2) The intermetallic thickness of the joints was affected by the wire feed rate and chemical composition of the filler wire. (3) Best tensile Strength of 188 N/mm^2 was observed for $AlSi_3Mn$,
5.	Babu et al. (2019)	1.AISI321 Austenitic Steel 2.AA2219 Aluminum Alloy	AA 4047 Filler wire of diameter 1.2mm	Thickness of both the sheets - 3mm Gas flow rate - 15L/min Current - 70A Speed - 400mm/min	(1) The experimental result concluded that acceptable quality of weld joint was produced by friction surfacing aluminum alloy coating on stainless steel before CMT welding. (2) Further, the results reported that as the alloy

				Before CMT welding stainless steel sheet was friction surfaced with aluminum alloy of different thickness ranging from 0.3mm to 1.2mm	coating increases from 0.3 mm to 1.2 mm intermetallic thickness layer was found to be decreased from 5 microns to 0.4 microns which helps in reducing the problem of liquid wetting of aluminum alloy on stainless steel. (3) Joint produced with coating thickness 0.6 mm was found to withstand greatest tensile shear load 260 N/m. (4) Low strength of the joints with thin coating was due to the formation of a thicker intermetallic layer.
6.	Chen et al. (2019)	1. Q235 Low Carbon Steel 2. AA5052 Aluminum Alloy	ER5356 Al-Mg Filler Wire	Thickness of both the - sheets 2mm Gas flow rate - 15L/min Power – 3Kw Beam offset - 0.2, 0.4, 0.6, 0.8, 1 mm Welding Speed - 1.5m/min to 4 m/min	(1) The experimental results showed that maximum strength that a joint reported was 83.40 MPa. (2) The joint was reported to fractured in interfacial intermetallic layers. (3) As wire feed rate increased the brittle inter metallic layers got thicker

				Wire feed rate - 3.1, 4.1, 5.1 m/min Different sets of experiments were designed using Taguchi design method.	and hence the tensile strength decreased. (4) Further, the experimental result showed that intermetallic layers decreased as the welding speed and offset increased but shape of the weld was not reported satisfactory. Tensile strength also first increased than decreased.
7.	Yang et al. (2019)	1. Q235 Low Carbon Steel 2.AA5754 Aluminum alloy	ER4043 Filler wire of diameter 1.2 mm.	Thickness of Low carbon steel sheet - 1.2mm. Thickness of aluminum alloy sheet - 1.8 mm. Current – 67A to 69 A Voltage - 10.9V to 11.8V Speed – 3 mm/sec to 7 mm/sec Wire feed rate - 4m/min Different sets of experiments were performed.	(1) The experimental result concluded that at low heat input lower than 157J/mm only a single phase layer of $Al_{7.2}Fe_{1.8}Si$ is formed while at high heat input above 210J/mm $FeAlSi_3$ and $Al_{7.2}Fe_{1.8}Si$ both are formed. (2) Further, it was reported that at single zone low interfacial mismatch is obtained and hence high strength as compared to combination of zone formed due to high energy input. (3) For having a sound joint and good bonding the heat

					input should be kept low so that a thin interface layer of $Al_{7.2}Fe_{1.8}Si$ is maintained at interface zone
8.	Mou et al. (2019)	1. SS 304 2.Titanium alloy TC4	ERCuSi-A Filler wire	Thickness of both the - sheets 2mm Gas flow rate 25L/min Shielding gas – Argon (99.9%) Welding speed – 45cm/min Wire feed rate – 3.5m/min to 5.5m/min Welding current – 60A to 110A Welding Voltage 10.8V to 11.3V	(1). The experimental results concluded that joint strength of 294 MPa was reported to be highest at 5.5 m/min wire feed rate. (2) As the wire feed speed increases the thickness of Cu/Ti layer and ultimate strength also increased. (3) When low heat input was given wetting condition was found to be degraded and ultimate tensile strength was found to be at lower side when torch was offset to the TC4 sample plate side. (4) Further, the experimental results concluded bonding strength between Cu/Ti and Cu/Fe interfaces influenced the fracture mode.

Table 2.3. Literature Review of Published work on welding of Austenitic Stainless Steel by Other Processes

S. No.	Author and Year	Material Used	Process	Process Parameter	Results and Conclusion
1.	Bharwal et al. (2014)	SS202	Metal Inert Gas (MIG) Welding	Thickness of sheets 6mm. Current – 160 A Gas flow rate – 6L/min Welding speed – 2.5mm/sec	1. Maximum Tensile Strength of 610 MPa was obtained. 2. SS 202 can be utilized instead of SS 304. 3. Presence of austenite grains in the heat affected zone and in the parent metal
2.	Singh et al. (2019)	1. SS202 2. SS304	Metal Inert Gas (MIG) Welding	Current – 50A, 75A, 100A, Voltage – 15V, 18V, 20V Gas flow rate – 10L/min, 15L/min, 20L/min	1. Based on the Taguchi method L9 design matrix was made for obtaining optimized combination of process parameter for conducting experiments. 2. Parametric optimization was carried out using Taguchi S/N ratio optimization. 3. Larger the better S/N ratio was used to obtain the optimized process parametric combination for

					obtaining maximum value of strength. 4. Welding Voltage showed the most dominating effect on tensile strength followed by welding current.
3.	Ghosh et al. (2016)	316L Stainless steel	Metal Inert Gas (MIG) Welding	Thickness of plate – 3mm Current – 100A, 112A, 124A Gas flow rate – 10L/min, 15L/min, 20L/min Nozzle to tip distance – 9mm, 12mm, 15mm	1. Grey-based Taguchi method using L9 design matrix array was used for parametric optimization of MIG welding that was carried out by the researcher. 2. Larger the better S/N ratio criteria was used find the optimized process parameter for obtaining maximum value of UTS, YS and percentage elongation. 3. Current was found to be most significant process parameter affecting the value of above three properties in comparison to other process parameter.
4.	Gautam et al. [20]	SS202	Gas Metal Arc Welding GMAW	Thickness of plates – 6mm. Welding current – 120A to 240A	1. Taguchi's S/N ratio optimization tool was used to find the most optimized value of process parameter.

			using 308L filler wire	Welding Speed – 160mm/min to 180 mm/min Gas flow rate – 5L/min to 9L/min	2. Current was the most significant factor affecting the value of Tensile strength. 3. Superior value of tensile strength that was obtained was 800 MPa.
5.	Pradhan et al. (2019)	1. SS202 2. SS304	Metal Inert Gas (MIG) Welding and Tungsten Inert Gas (TIG) Welding	Thickness of the sheets – 6mm	1. SS 308 recommend filler wire. 2. Higher grain size was reported for TIG in comparison to MIG. 3. Value of process parameters plays and important role in determining the properties.
6.	Juang et al. (2002)	SS304	Metal Inert Gas (MIG) Welding	Thickness of the sheets – 1.5mm Current – 40A to 55A Welding speed – 13.5 cm/min to 15.0 cm/min Gas flow rate – 8L/min to 11L/min	1. Taguchi S/N ratio for optimization of response value and ANOVA analysis tool was used to determine which process parameter significantly affect the response value. 2. Front height back height of the weld pool was analyzed using smaller the better S/N ratio tool.

7.	Biswas et al. (2018)	1. SS304 2. 45C8	Gas Metal Arc Welding	Thickness of sheets 3mm Current – 140A to 160A Welding speed – 4-6mm/sec Voltage – 24V to 26V Gas flow rate – 6L/min to 10L/min	1. The experimental result reported the maximum value of Ultimate tensile strength, Yield stress and that were obtained was 722 MPa, 640 MPa respectively. 2. For finding optimized parameter for obtaining maximum value of UTS and Yield Stress Taguchi Higher the better S/N ratio criteria was used.

2.5 CONCLUSION DRAWN FROM LITERATURE REVIEW

The effect different process parameter such as welding speed, current, voltage, gas flow rate, welding voltage, Arc length correction factor, Contact tip to work distance (CTWD) on the microstructural and mechanical properties of weld bead while joining different grades of steels with similar by Cold Metal Transfer Process as investigated and explained by researcher in there published work have been discussed in this research work. Further welding of Austenitic Stainless Steel grades such as SS202, SS304 and SS316 by other arc welding process such as MIG welding and TIG welding has also been discussed as reported by the researchers in their work. Following conclusion are drawn from the above literature survey.

1. Thickness of the sheets and type of base material determines heat input as given by equation 2.1 [Dhobale et al. (2015)] which is dependent on the current, voltage and welding speed value. Higher value of current is required for plates of higher thickness. However other parameter such as welding speed should also be controlled depending on the thickness, too high or too low speed results in inadequate penetration.

$$\text{Heat input (Q)} = \eta \frac{V \times I}{S} \quad (2.1)$$

where, η is welding efficiency, V is voltage, I is current and S is welding speed

2. The heat input affects the microstructure of the weld, as different properties of weld bead are influenced such as austenite/ ferrite balance. More over a sufficient amount of heat is required for passing the zinc bubble from the weld while welding of zinc of coated steel by Cold Metal Transfer Welding process. Further, the grain refinement is also controlled by heat input.
3. The Cold Metal transfer process makes it possible to give controlled value of heat that is to be given for the welding of base plate because of swift retraction of filler wire during short circuit process. Controlled input of Heat is very crucial parameter for obtaining optimum weld bead properties.
4. CMT arc mode gives best bead stability, spatter free weld and least heat affected zone as compared to Pulsed arc mode and Standard arc mode.
5. The mechanical properties such as Ultimate Tensile Strength, Yield Strength and Percentage Elongation are dependent on the process parameter of welding, best results are reported for CMT welding of stainless steels as compared to other arc welding process.
6. Choice of filler wire is also important for obtaining better results during CMT welding. The filler wire should have compatible chemical and mechanical properties as compared to the base material.
7. Choice of shielding gas is also an important parameter during CMT welding. Shielding gas protects the molten weld pool from atmospheric gases. Shielding gas should be chosen depending on the base material and adequate amount of gas flow rate should be provided. Without shielding gas porosity and other defects were reported.

8. For getting optimum parametric combination Taguchi design array is implemented and for optimizing the response value Taguchi S/N ratios are used.

2.6 RESEARCH GAP

Cold Metal Transfer Welding Technology has explored many areas in welding since its introduction and redefined the welding industries. Still a lot of work is to be done. Some of them are as follows –

1. There is very less literature available for welding of thin austenitic stainless steels sheets of thickness 2mm by CMT welding process. Process parameter are yet to be defined for the welding of sheets of such less thickness.
2. For SS202 material which has tremendous application and desirable properties as discussed above in chapter 1, very less literature is available in the domain of welding by CMT welding process
3. Study of influence of Pulse dynamic correction factor on the weld bead properties of stainless steel during Cold Metal transfer welding is still a domain touched by few researchers. The pulse dynamic correction factor influences the detachment rate of the droplet.
4. Effect of other process parameter on Heat affected zone, grain refinement, mechanical properties, microstructural properties of the weld bead during welding of SS202 thin sheets by CMT welding are also the topic of interest for the researchers.
5. CMT welding of SS202 based on three process parameter current, welding speed and Pulse dynamic correction factor together, and their effect on Weld bead properties is yet to be studied by the researchers.

6. Ultrasonic vibration assisted CMT welding of thin sheets SS202 steel based on three process parameter current, welding speed, and Pulse dynamic correction factor and their effect on weld bead properties is still not explored by the researchers.

CHAPTER 3 EXPERIMENTAL PROCEDURE

3.1 MATERIAL AND METHODS

Experimental trials were carried out on SS202 plates of dimension 100mm × 60mm × 1.58mm. The chemical composition (%wt.) of SS202 base plate is displayed in Table 3.1 below. SS308 electrode wire of 1.2 mm diameter was used as filler wire which is having compatible composition and mechanical characteristics as SS202 [Gautam et al. (2018)]. The samples were welded by cold metal transfer welding process using TPS 400i CMT welding machine (by Fronius) as displayed in Figure 3.1. The samples were cleaned first with acetone in order to eliminate the surface films and dirt if any and then, the samples were tightly clamped on the welding table using fixtures in order to avoid the bending of the plates during the welding. A shielding gas with 98 % argon and 2 % CO_2 composition was used for conducting the experiment. [Liao M.T. et al. (2008)] reported that shielding gas shelter the welded pool from atmospheric gases (e.g. oxygen and nitrogen) which influences the microstructure of the stainless steel weldment. Increasing the CO_2 percentage in the mixture of Argon and CO_2 increases the carbon content in weld deposits and also the spatter rates.

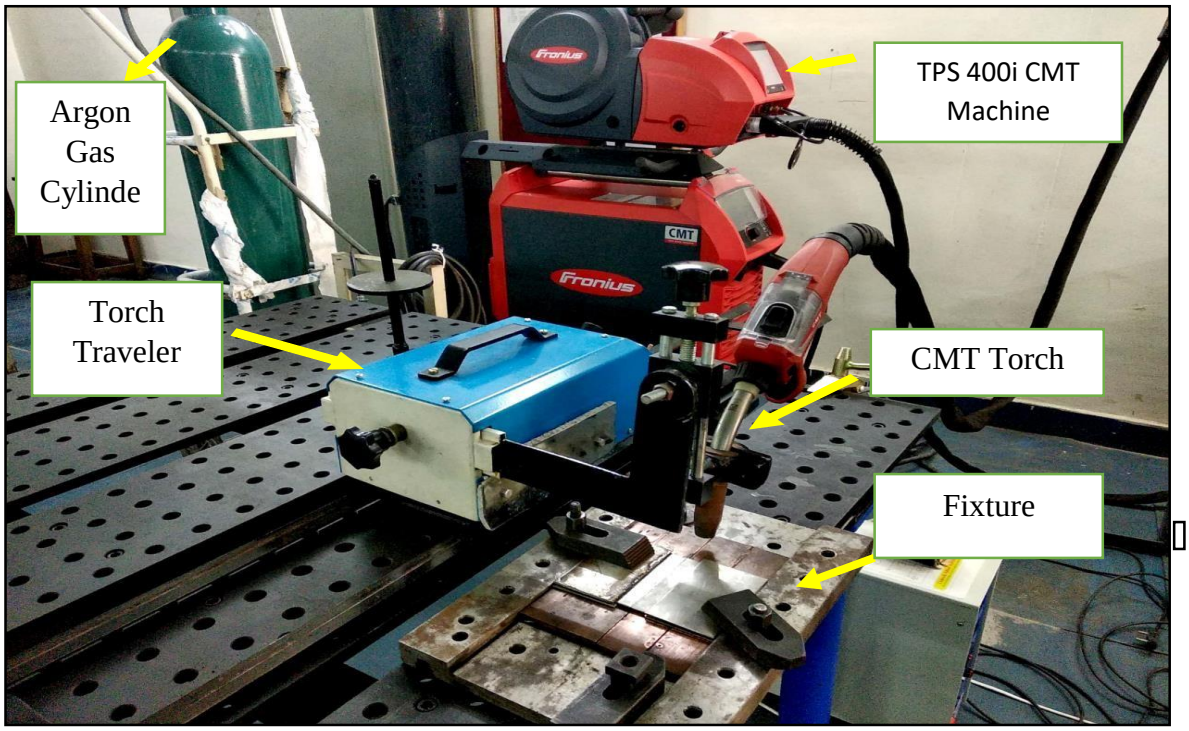

Figure 3.1: Experimental Setup for CMT Welding Process

Table 3.1. Chemical composition (%wt.) of SS 202 base plate material

Fe	C	Si	Mn	P	S	Cr	Mo	Ni	Co	Cu
73.9	0.103	0.490	10.5	0.0730	0.0179	12.8	0.303	0.205	0.0279	1.39

3.2 PROCESS PARAMETER

After in depth analysis of published work as mentioned in chapter 2 three independent process parameter Current, Welding Speed and Pulse dynamic correction factor were set for first few trail experiment. The weld bead and plates after each trial run was analyzed visually to check for the burn through and distortions of the base plates. Finally, three different optimized values were obtained for each process parameter. Contact tip to work distance (CTWD) and shielding gas flow rate were kept constant at 10mm and 15 L/min for each experiment respectively. Using Taguchi's Design of experiment best optimized parametric combination of process parameter using MINITAB 19 Software was found as shown in figure 3.2. Based on Taguchi's L9 design of experiment array total nine parametric combinations had been designed using three different levels of Pulse dynamic correction factor, current and welding speed. Table 3.2 shows the values of three different welding process parameter and their levels and Table 3.3 shows the design matrix. In this research the symbol C is used for Current, S for welding speed and P for Pulse dynamic factor. Actual value of process parameter based on Taguchi's design of experiment array is displayed in Table 3.4.

Table 3.2. Value of Process Parameter and their levels based on Taguchi's design of experiment

Process Parameter	Welding Current	Welding Speed	Pulse Dynamic Correction factor (PDC)
Unit	Ampere	mm/sec	N/A
Symbols	C	S	P
Level 1	80	3	-10
Level 2	100	4	0
Level 3	120	5	+10

Table 3.3. Taguchi's L9 design of experiment matrix

Sample No.	Welding Process Parameters		
	Welding Current (A)	Welding Speed (mm/sec)	Pulse Dynamic Correction Factor (PDC)
1	1	1	1
2	1	2	2
3	1	3	3
4	2	1	2
5	2	2	3
6	2	3	1
7	3	1	3
8	3	2	1
9	3	3	2

Table 3.4 Taguchi's L9 - Orthogonal Array with actual value of Process Parameters

Sample No.	Welding Process Parameter		
	Welding Current (A)	Welding Speed (mm/sec)	Pulse Dynamic Correction factor (PDC)
1	80	3	-10
2	80	4	0
3	80	5	+10
4	100	3	0
5	100	4	+10
6	100	5	-10
7	120	3	+10
8	120	4	-10
9	120	5	0

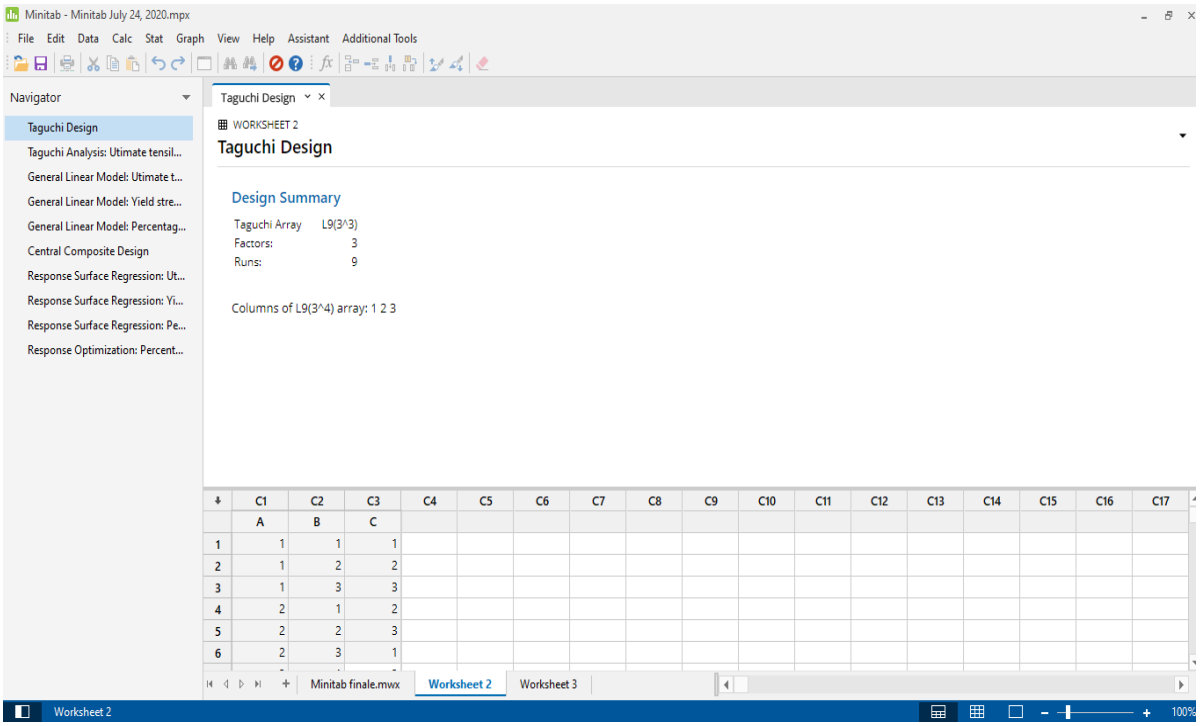

Figure 3.2: Taguchi L9 Design of experiment Interface on Minitab 19 Software

After obtaining the optimized process parametric combination as discussed above. the CMT welding on the SS202 sheets was performed. Figure 3.3 to Figure 3.11 displays the CMT welded sample based on optimized process parameter individually. Figure 3.12 shows the combine image of all the 9 samples welded in this research work. Table 3.5 to 3.13 displays the process parameter matrix for individual samples. Voltage is dependent process parameter depends on the current value and the value of voltage is obtained from the CMT welding machine. Similarly wire feed rate in mm/min is a dependent process parameter and hence, the value is obtained from the machine. Arc length correction factor ALC is kept at 0 % for all the welded samples.

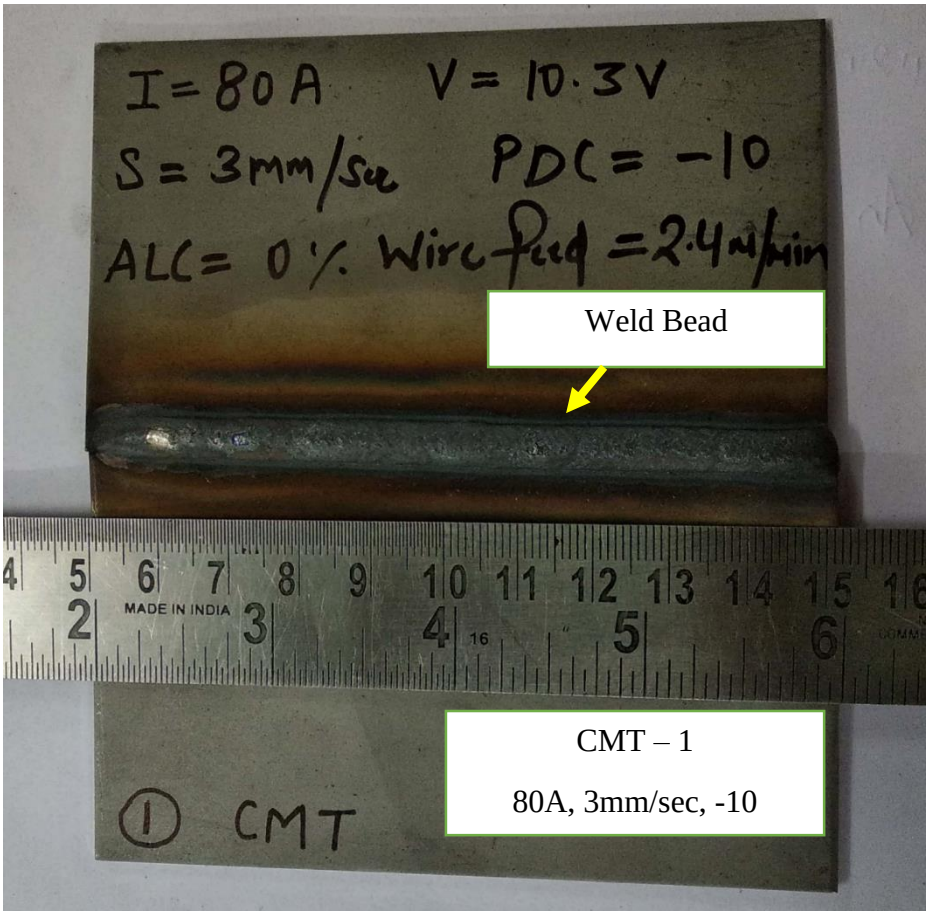

Figure 3.3: Image of CMT welded SS202 Sample 1 of thickness 1.58 mm

Table 3.5 Process Parameter Matrix for CMT welding of SS202 Sample 1

Process Parameter	Value
Current (A)	80 A
Welding Sped (mm/sec)	3 mm/sec
Pulse Dynamic Correction Factor	- 10
Voltage (V)	10. 3 V
Wire feed rate (m/min)	2.4 m/min
Arc length Correction Factor (%)	0 %
Contact Tip to work distance (mm)	10 mm

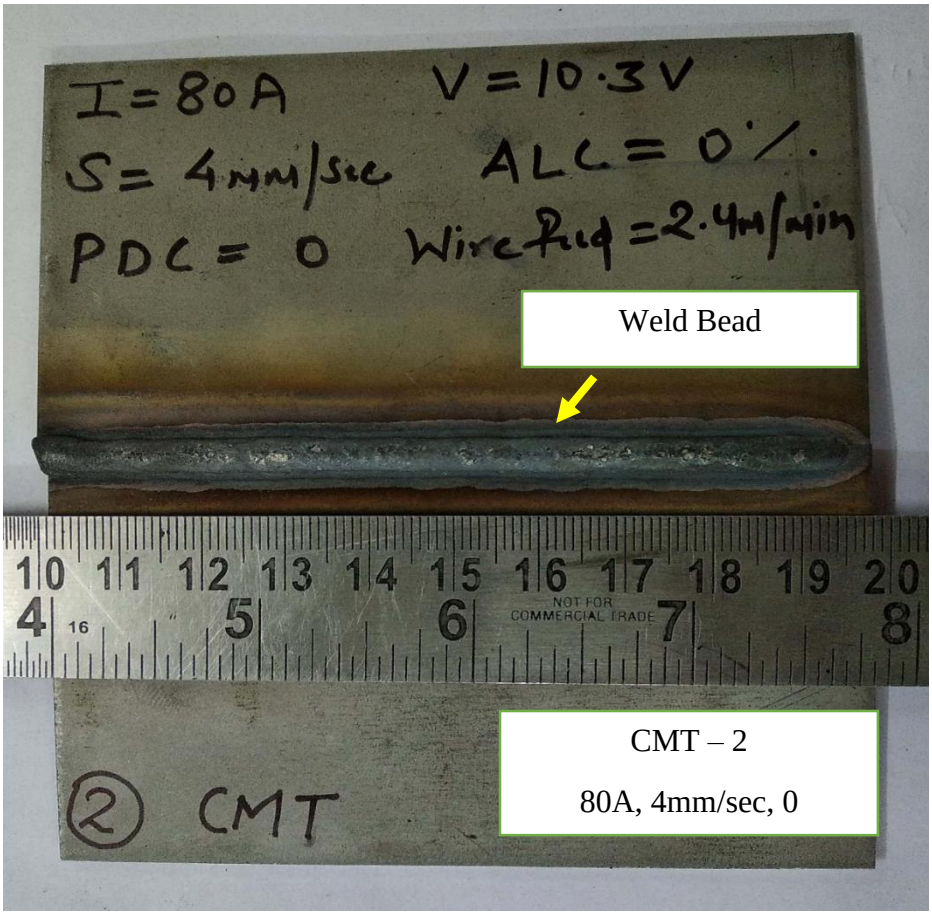

Figure 3.4: Image of CMT welded SS202 Sample 2 of thickness 1.58 mm

Table 3.6. Process Parameter Matrix for CMT welding of SS202 Sample 2

Process Parameter	Value
Current (A)	80 A
Welding Sped (mm/sec)	4 mm/sec
Pulse Dynamic Correction Factor	0
Voltage (V)	10.3 V
Wire feed rate (m/min)	2.4 m/min
Arc length Correction Factor (%)	0 %
Contact Tip to work distance (mm)	10 mm

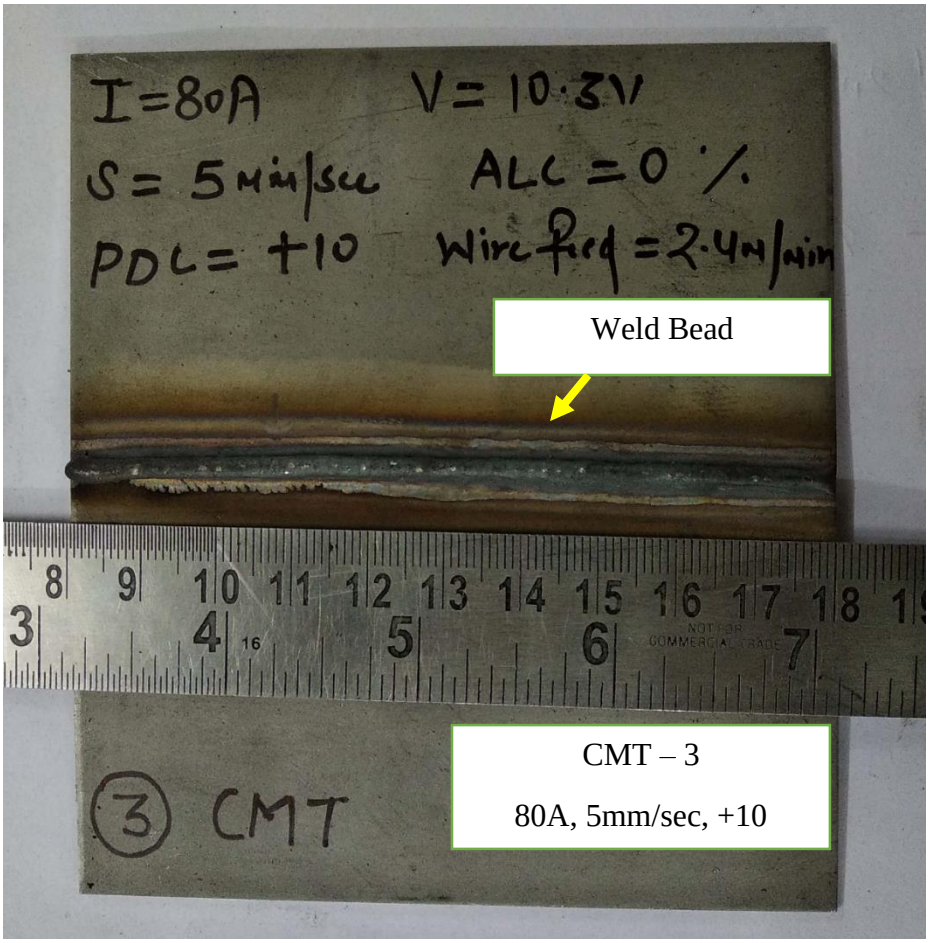

Figure 3.5: Image of CMT welded SS202 Sample 3 of thickness 1.58 mm

Table 3.7 Process Parameter Matrix for CMT welding of SS202 Sample 3

Process Parameter	Value
Current (A)	80 A
Welding Sped (mm/sec)	5 mm/sec
Pulse Dynamic Correction Factor	+10
Voltage (V)	10.3
Wire feed rate (m/min)	2.4 m/min
Arc length Correction Factor (%)	0 %
Contact Tip to work distance (mm)	10 mm

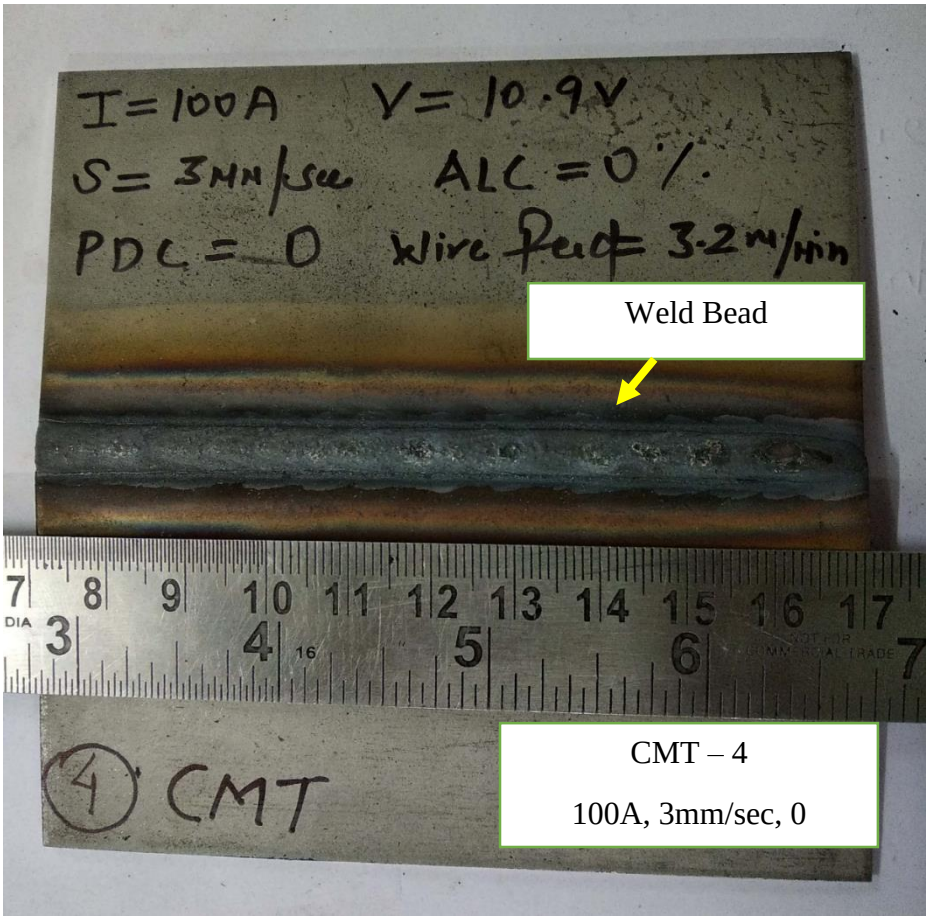

Figure 3.6: Image of CMT welded SS202 Sample 4 of thickness 1.58 mm

Table 3.8. Process Parameter Matrix for CMT welding of SS202 Sample 4

Process Parameter	Value
Current (A)	100 A
Welding Sped (mm/sec)	3 mm/sec
Pulse Dynamic Correction Factor	0
Voltage (V)	10.9 V
Wire feed rate (m/min)	3.2 m/min
Arc length Correction Factor (%)	0 %
Contact Tip to work distance (mm)	10 mm

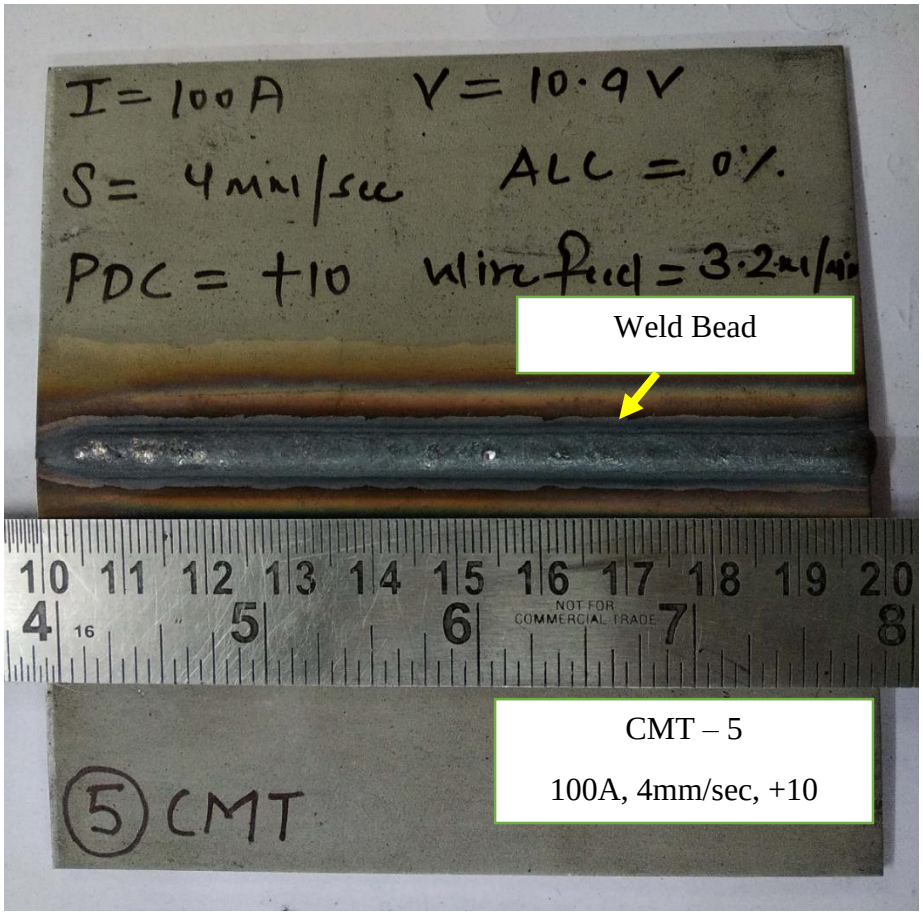

Figure 3.7: Image of CMT welded SS202 Sample 5 of thickness 1.58 mm

Table 3.9. Process Parameter Matrix for CMT welding of SS202 Sample 5

Process Parameter	Value
Current (A)	100 A
Welding Sped (mm/sec)	4 mm/sec
Pulse Dynamic Correction Factor	+10
Voltage (V)	10.9
Wire feed rate (m/min)	3.2 m/min
Arc length Correction Factor (%)	0 %
Contact Tip to work distance (mm)	10 mm

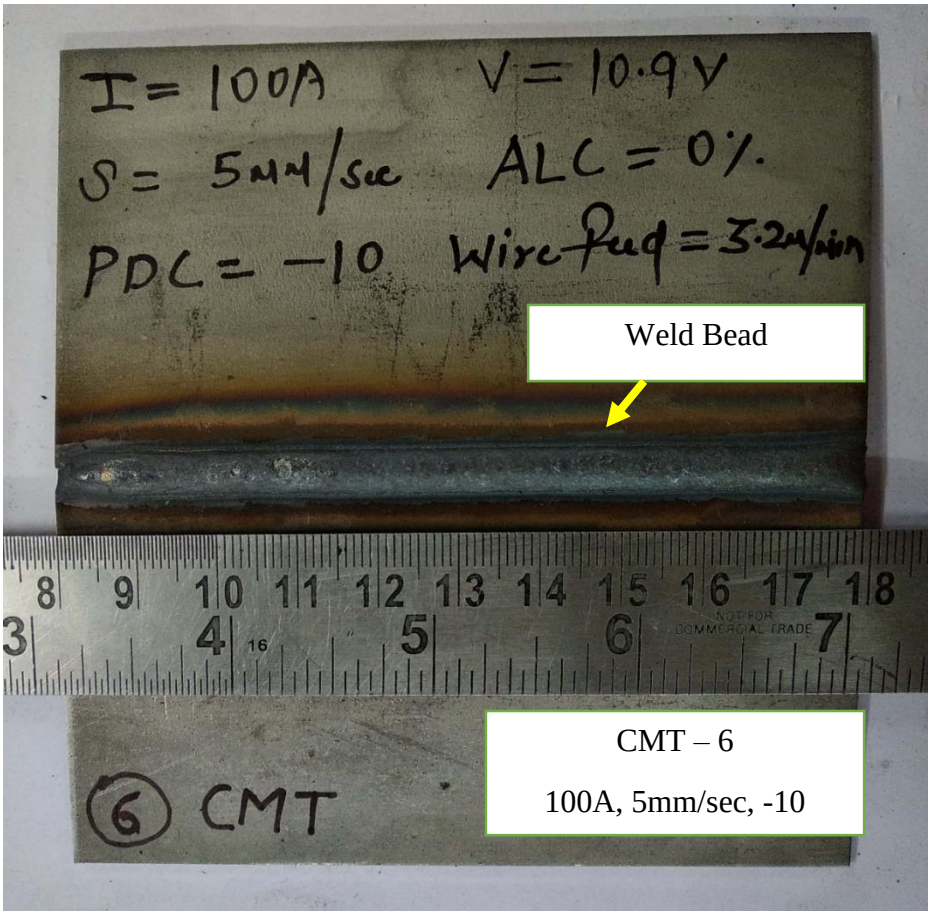

Figure 3.8: Image of CMT welded SS202 Sample 6 of thickness 1.58 mm

Table 3.10. Process Parameter Matrix for CMT welding of SS202 Sample 6

Process Parameter	Value
Current (A)	100 A
Welding Sped (mm/sec)	5 mm/sec
Pulse Dynamic Correction Factor	-10
Voltage (V)	10.9 V
Wire feed rate (m/min)	3.2 m/min
Arc length Correction Factor (%)	0 %
Contact Tip to work distance (mm)	10 mm

Figure 3.9: Image of CMT welded SS202 Sample 7 of thickness 1.58 mm

Table 3.11. Process Parameter Matrix for CMT welding of SS202 Sample 7

Process Parameter	Value
Current (A)	120 A
Welding Sped (mm/sec)	3 mm/sec
Pulse Dynamic Correction Factor	+10
Voltage (V)	11.8 V
Wire feed rate (m/min)	4.1 m/min
Arc length Correction Factor (%)	0 %
Contact Tip to work distance (mm)	10 mm

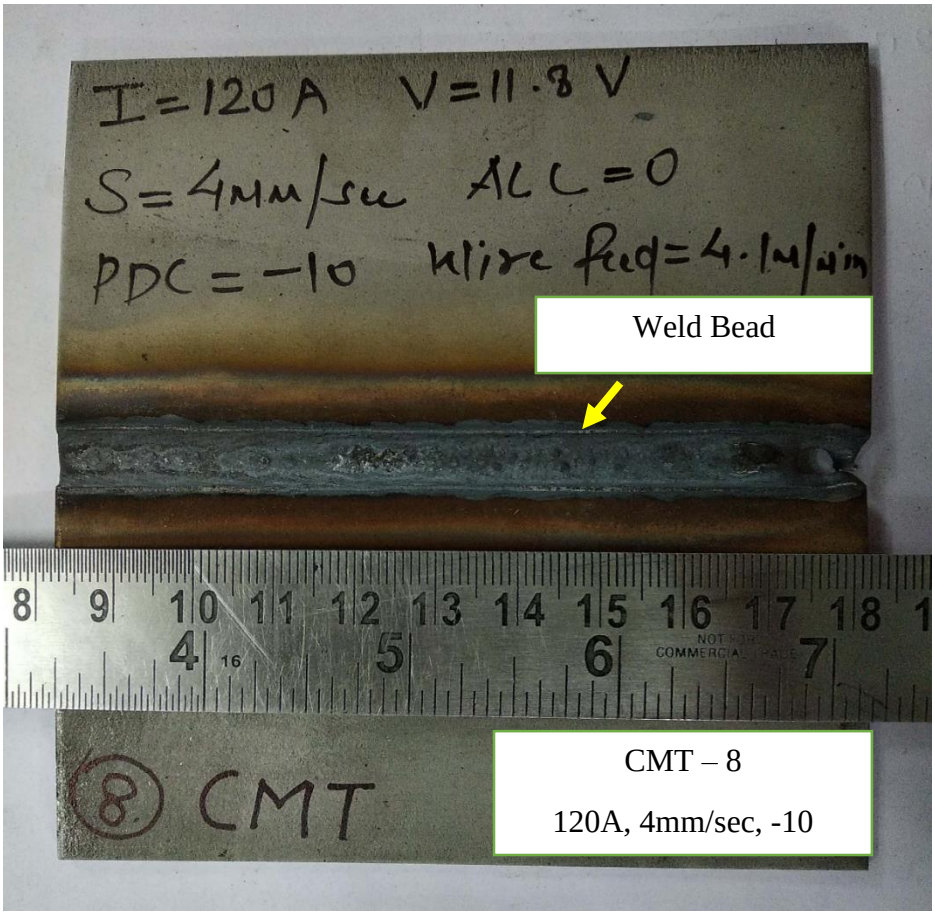

Figure 3.10 Image of CMT welded SS202 Sample 8 of thickness 1.58 mm

Table 3.12. Process Parameter Matrix for CMT welding of SS202 Sample 8

Process Parameter	Value
Current (A)	120 A
Welding Sped (mm/sec)	4 mm/sec
Pulse Dynamic Correction Factor	-10
Voltage (V)	11.8 V
Wire feed rate (m/min)	4.1 m/min
Arc length Correction Factor (%)	0
Contact Tip to work distance (mm)	10 mm

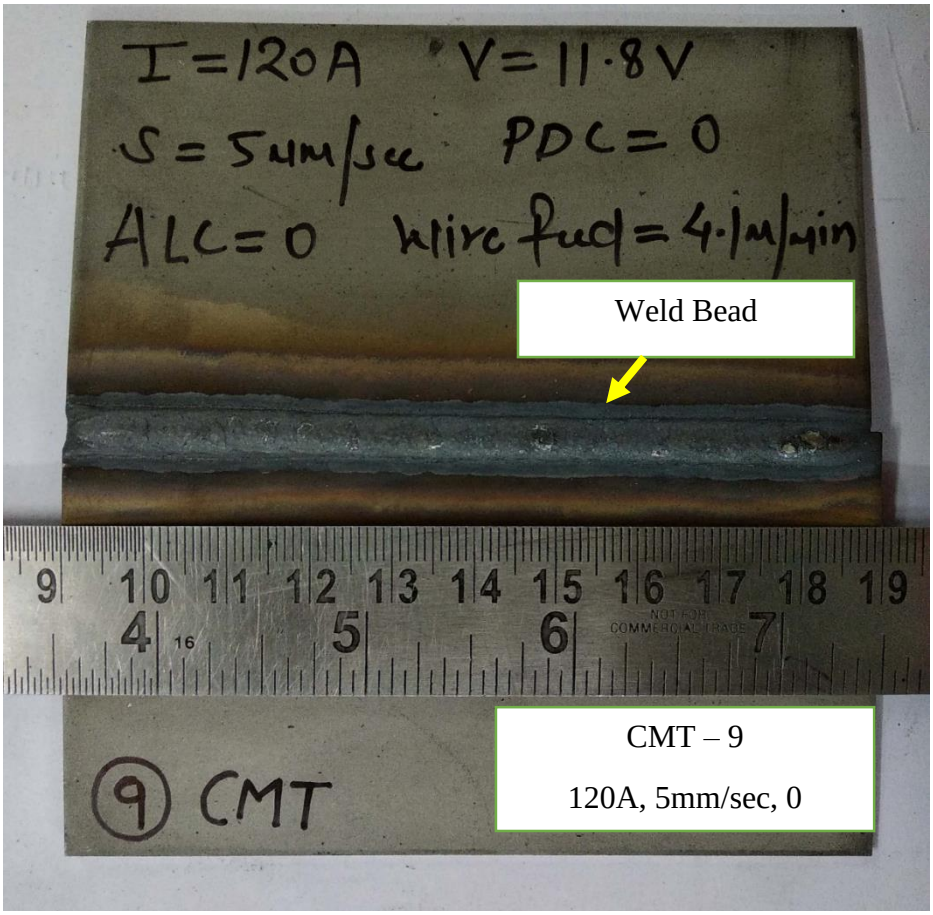

Figure 3.11: Image of CMT welded SS202 Sample 9 of thickness 1.58 mm

Table 3.13 Process Parameter Matrix for CMT welding of SS202 Sample 9

Process Parameter	Value
Current (A)	120 A
Welding Sped (mm/sec)	5 mm/sec
Pulse Dynamic Correction Factor	0
Voltage (V)	11.8 V
Wire feed rate (m/min)	4.1 m/min
Arc length Correction Factor (%)	0 %
Contact Tip to work distance (mm)	10 mm

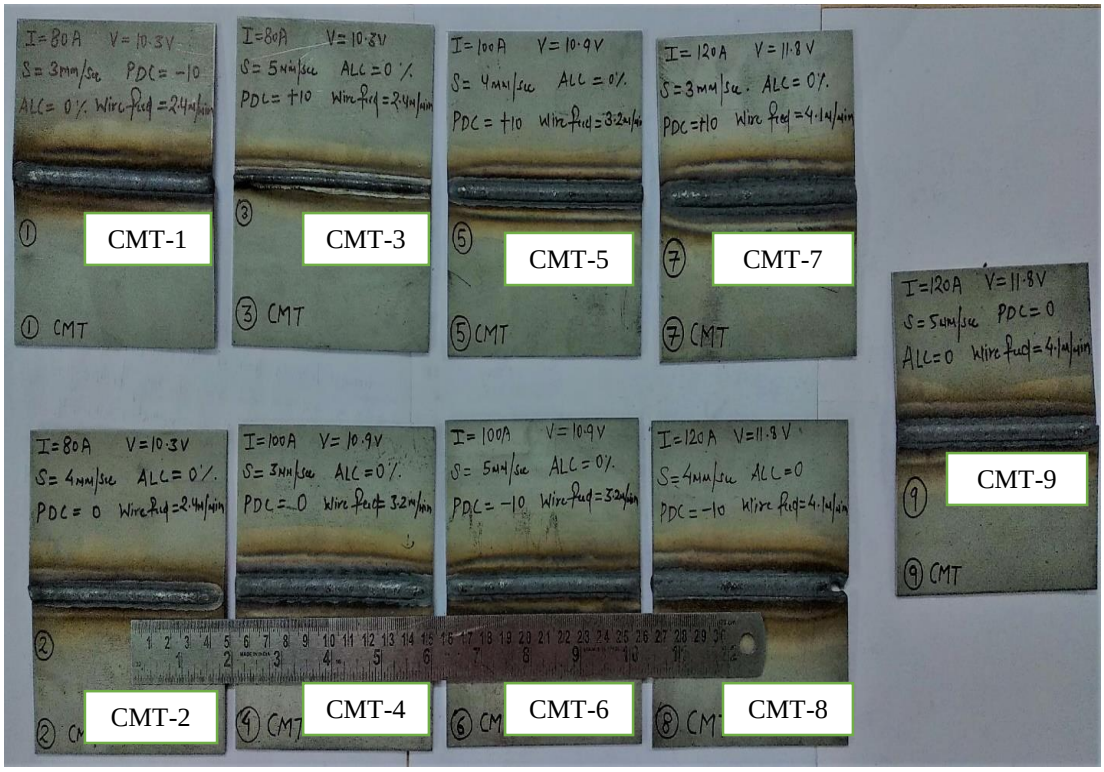

Figure 3.12: Image of all the 9 samples Welded by CMT welding Process

3.3 TENSILE TESTING

Tensile testing is done to determine the Tensile strength of the welded samples. Further Yield strength and Percentage Elongation can also be found. The Yield strength shows the load bearing capacity of the specimens before the permanent deformation occurs. Welded samples are shown in figure 3.12. From the welded samples optimum size specimens as shown in figure 3.13 were cut with specific dimensions using wire cut EDM process with reference to ASTM standard. The specimens were cut into 100mm length with the sub size of gauge length of 32mm and width 6mm. The Yield Strength (YS), Ultimate Tensile Strength (UTS), and Percentage Elongation value of the welded specimens were determined using TINIUS OLSEN UTM H50KS of 50 KN shown in figure 3.14 by applying load at fixed extension rate of 1 mm/min at room temperature.

Figure 3.13: CMT welded specimens test specimens for tensile testing

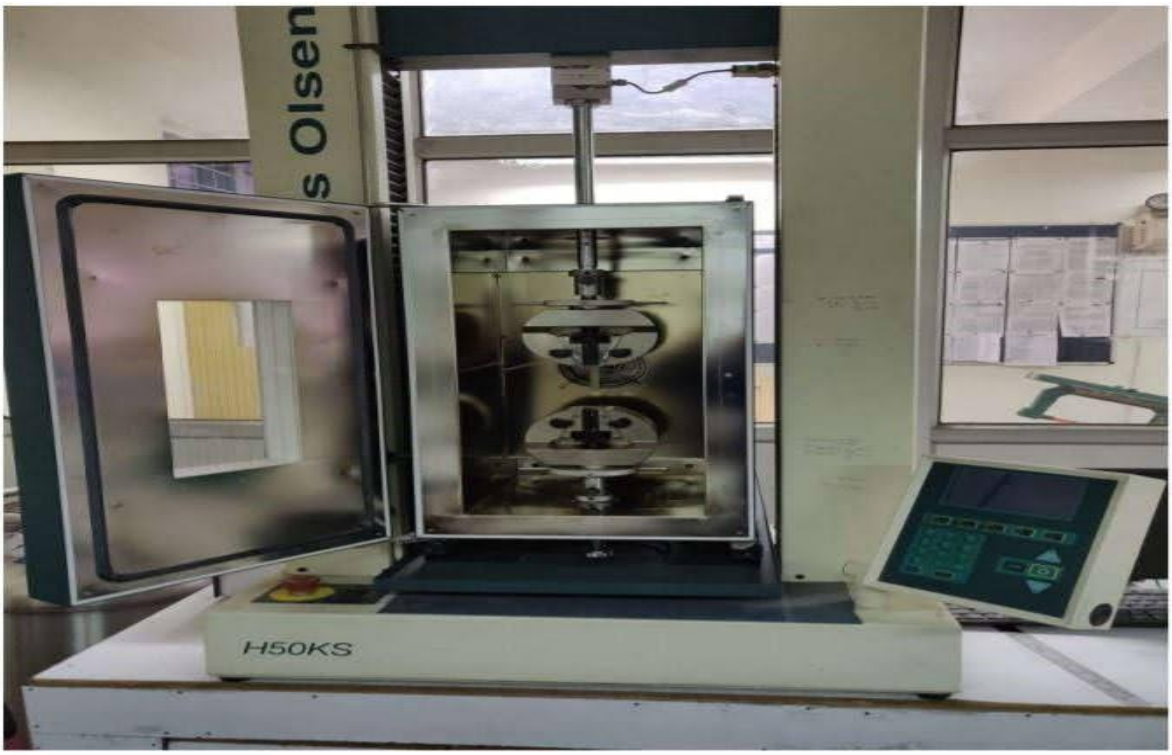

Figure 3.14: TINIUS OLSEN UTM H50KS of 50 KN for tensile Testing

CHAPTER 4 RESULTS AND DISCUSSION

4.1 TENSILE TESTING RESULTS

The Yield Strength (YS), Ultimate Tensile Strength (UTS), and Percentage Elongation value of the welded specimens were determined as in section 3.3 as discussed above. Table 4.1 shows the value of three for all the 9 samples at different process parameters. [Gautam et al. (2018)] reported maximum tensile strength of 800 MPa for SS202 welded sample using GMAW process. In this research work from the experimental result highest tensile strength of 871 MPa for sample 8 was obtained at process parameter C3S2P1 (at 120A Current, 4 mm/sec Welding Speed and -10 Pulse dynamic factor). [Kannan et al. (2019)] reported maximum Yield strength of 221 MPa for cold metal transfer welded 2mm thick austenitic stainless steel sheets. Maximum Yield Strength and Percentage elongation for MIG welded austenitic stainless steel sheets of 3mm as reported by [Ghosh et al. (2016)] were 322.7 MPa, and 65.04 % respectively. In this study superior value of yield strength of 379 MPa for the sample 2 was recorded at C1S2P2 process parameter (at 80A Current, 4mm/sec Welding Speed and 0 Pulse dynamic factor) and maximum percentage elongation of 65.9 % was recorded for sample 8 at process parameter C3S2P1 (at 120A Current, 4 mm/sec Welding Speed and -10 Pulse dynamic factor). The welding efficiency was found to be more than 100% as tensile strength of the SS202 parent sample [Keshari et al. (2019) and Pradhan et al. (2019)] is low as compared to tensile strength obtained for the welded sample as discussed above. The stress-strain curve for the CMT welded samples 1, 2, 4, 6, 7 and 8 together is shown in figure 4.1. Figure 4.2 shows stress stain curve for CMT welded samples 1, 2, 4, 6, 7 and 8 individually. Percentage elongation indicates the tensile ductility of the material [Takeda et al. (2017)]. All the welded samples showed more than 50 % percentage elongation and maximum a yield strength of 379 MPa. Value of yield strength which is determined at 0.2% offset or 0.2 percent strain is important in the engineering application where deflection is considered. [Faridmehr et al. (2014)].

Table 4.1: Process parameter and Response table for all the 9 samples

Sample No.	Welding Process Parameter			Responses		
	Current (A)	Speed (mm /sec)	Pulse Dynamic Correction Factor (PDC)	Ultimate Tensile Strength (MPa)	Yield Strength (MPa)	Percentage Elongation (%)
1	80	3	-10	807	204	54.4
2	80	4	0	817	379	58.8
3	80	5	+10	750	260	52.4
4	100	3	0	860	365	59.8
5	100	4	+10	742	279	50.8
6	100	5	-10	782	198	53.2
7	120	3	+10	763	217	50.4
8	120	4	-10	871	209	65.9
9	120	5	0	807	149	64.4

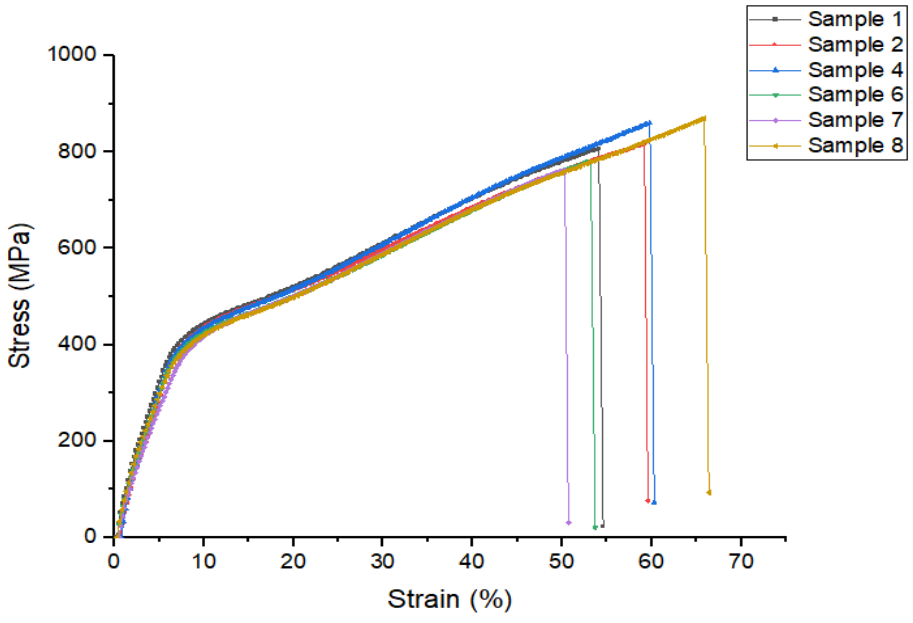

Figure 4.1: Typical Stress-Strain Curve for Welded Samples.

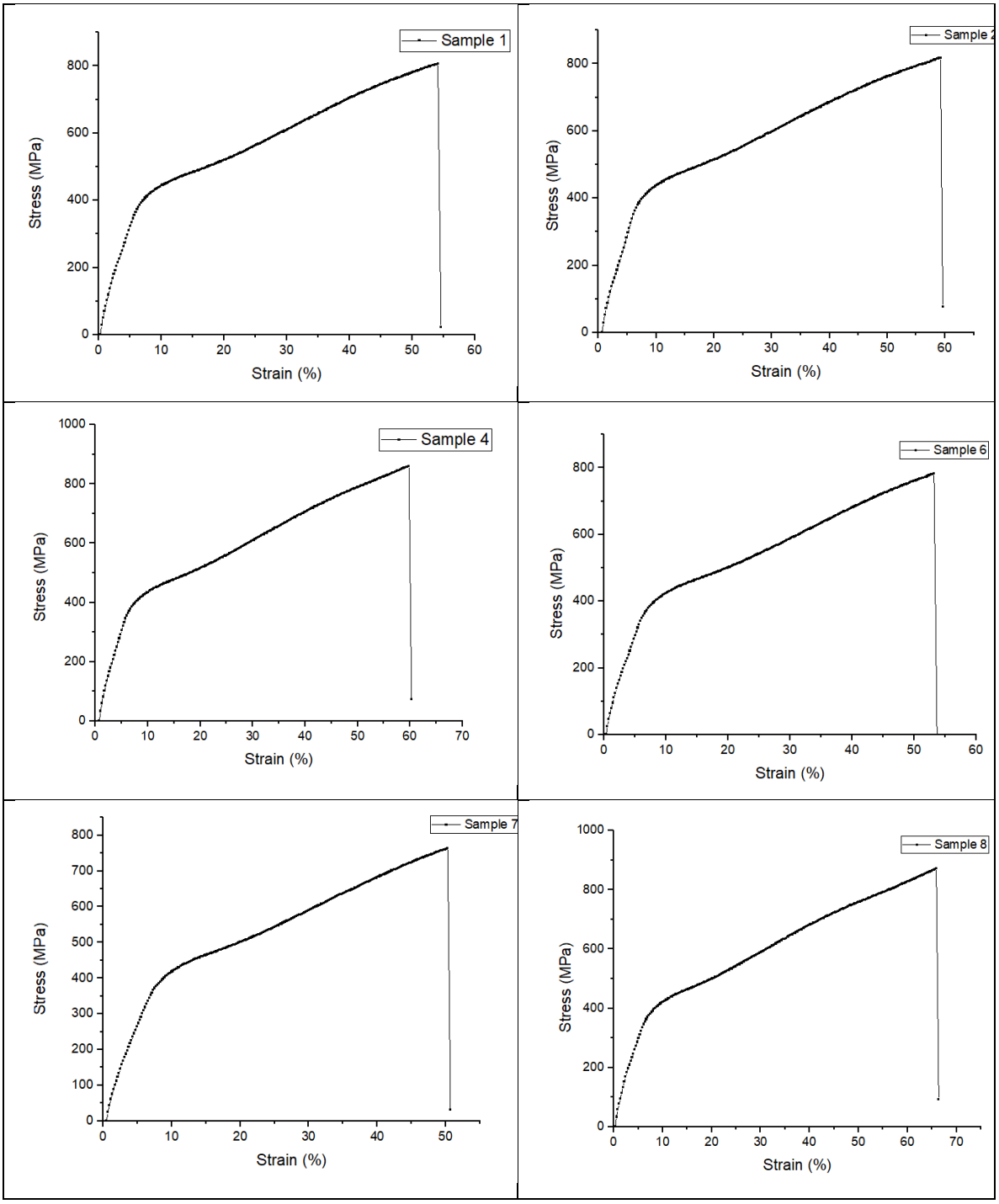

Figure 4.2. Typical Stress-Strain curve for the welded specimens (Sample 1, Sample 2, Sample 4, Sample 6, Sample 7, Sample 8)

4.2 OPTIMIZATION OF RESULTS BY TAGUCHI METHOD

The experimental results were analyzed by Taguchi's Method using MINITAB 19 software as shown in figure 4.3 Signal-to-Noise (S/N) ratio is a numerical measure of performance taking both average and inconsistency into account used in the Taguchi method [Ghosh et al. (2016)]. There are three typical S/N ratios that are used and evaluation is done based on the requirement of the process or product to be optimized. The three different S/N ratio are:

(a) Smaller –the-better: S/N ratio $= -10\log_{10}\frac{1}{n}\sum_{i=1}^{n} Y^2$ (1)

(b) Nominal-the-best: S/N ratio $= -10\log_{10}(s^2)$ (2)

(c) Larger-the-better: S/N ratio $= -10\log_{10}\frac{1}{n}\sum_{i=1}^{n}\frac{1}{Y^2}$ (3)

where Y = value of responses obtained experimentally for every factor-level combination, n is the no. of responses, s is the standard- deviation of n number of observation.

To get the maximum value of Tensile Stress, Yield Stress and Percentage Elongation Larger-the-better S/N ratio criteria was used. S/N ratios for ultimate tensile strength using larger the better criteria are mentioned in Table 4.2. Figure 4.4 shows that most optimum parametric combination for obtaining maximum ultimate tensile strength is C3S1P2 that is level-3 for current, level-1 for speed and level-2 for Pulse dynamic correction factor (that is 120A current, 3 mm/sec speed and 0 Pulse dynamic correction factor). Table 4.3 displays response table for S/N ratios for Maximum Yield Stress using larger the better criteria. Figure 4.5 shows the most optimum value of respective process parameter for obtaining maximum yield stress. Most optimum parametric combination is C2S2P2 that is level-2 for current, level-2 for speed and level-2 for Pulse dynamic correction factor (that is 100A current, 4 mm/sec speed and 0 Pulse dynamic correction factor). Table 4.4 displays response table for S/N ratios for Maximum Percentage elongation using larger the better criteria. From Figure 4.6 it can be concluded that most optimum process parameter for obtaining maximum value of percentage elongation is C3S2P2 that is Level-3 for current, level-2 for welding speed and level-2 for Pulse dynamic correction factor (that is 120A current, 4 mm/sec speed and 0 Pulse dynamic correction factor). Table 4.5. displays response table for S/N ratio considering Maximization of Yield Strength (YS), Ultimate tensile strength (UTS), and Percentage

Elongation. Figure 4.7 displays that for obtaining most optimum value of three simultaneously for a single sample the most optimized process parameter is C3S2P2 that is Level-3 for current, level-2 for welding speed and level-2 for Pulse dynamic correction factor (that is 120A current, 4 mm/sec speed and 0 Pulse dynamic correction factor). Current shows highest ranking for Yield Stress. Pulse dynamic correction factor showed highest ranking for Ultimate tensile strength and Percentage elongation. As high value of Pulse dynamic correction factor results in low value of detachment current and hence low heat input, and low value of Pulse dynamic correction factor results in larger detachment current value and hence more heat input [Rajeev et al. (2019)]. At 0 Pulse dynamic correction factor most significant result were reported as discussed above, which indicates both fast and slow rate of droplet detachment at constant energy level affects the weld bead properties.

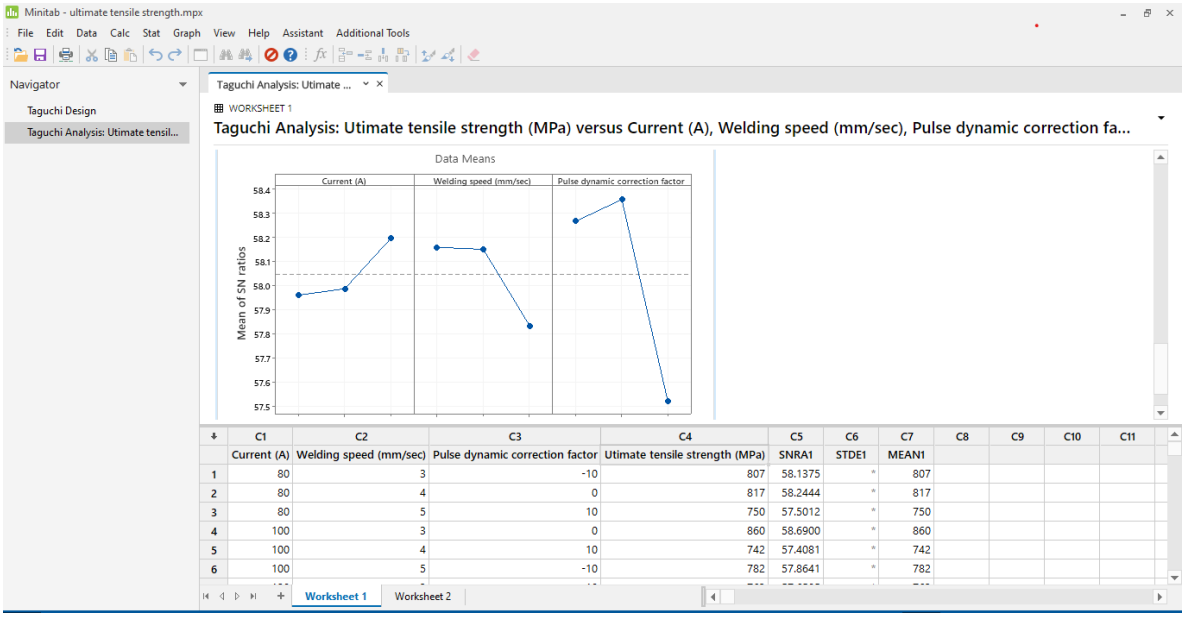

	C1	C2	C3	C4	C5	C6	C7	C8	C9	C10	C11
	Current (A)	Welding speed (mm/sec)	Pulse dynamic correction factor	Utimate tensile strength (MPa)	SNRA1	STDE1	MEAN1				
1	80	3	-10	807	58.1375	*	807				
2	80	4	0	817	58.2444	*	817				
3	80	5	10	750	57.5012	*	750				
4	100	3	0	860	58.6900	*	860				
5	100	4	10	742	57.4081	*	742				
6	100	5	-10	782	57.8641	*	782				

Figure 4.3: Taguchi Higher the better S/N ratio interface in MINITAB 19 software

Table 4.2: Response -Table for S/N Ratios for Maximum Ultimate tensile strength (UTS)

Level	Current (A)	Welding Speed (mm/sec)	Pulse Dynamic Correction Factor (PDC)
1	57.96	58.16	58.27
2	57.99	58.15	58.36
3	58.20	57.83	57.52
Delta	0.24	0.33	0.84
Rank	3	2	1

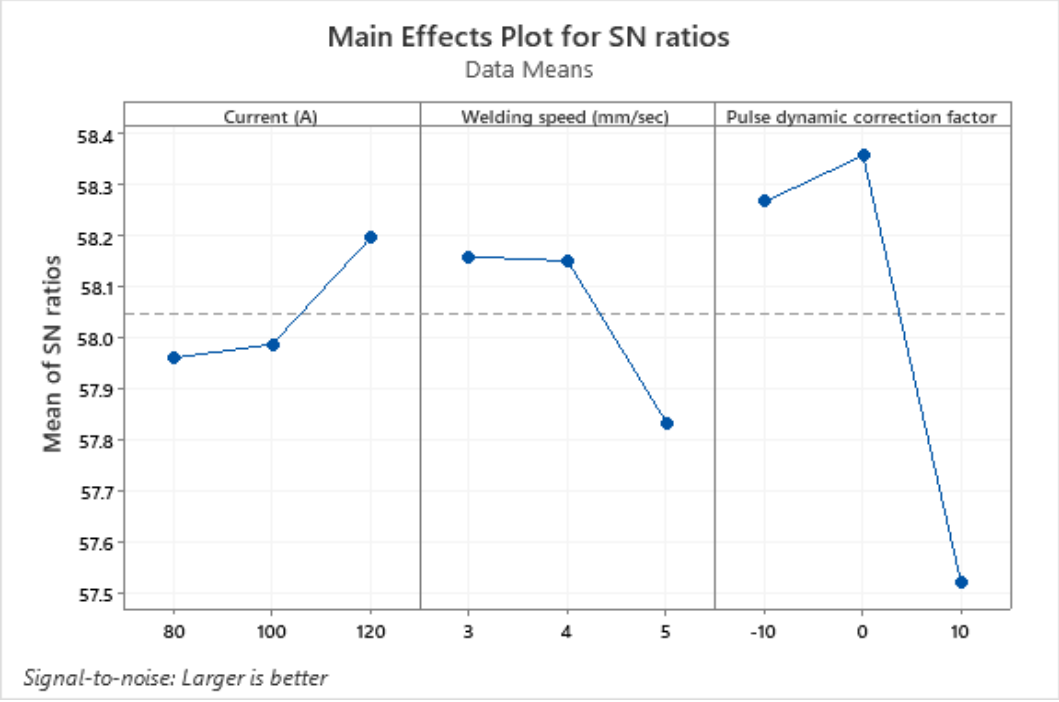

Figure 4.4: Mean S/N ratio graph for Ultimate tensile strength (UTS)

Table 4.3: Response - Table for S/N Ratios for Maximum Yield Stress (YS)

Level	Current (A)	Welding Speed (mm/sec)	Pulse Dynamic Correction Factor (PDC)
1	48.69	48.06	46.18
2	48.70	48.96	48.76
3	45.53	45.90	47.98
Delta	3.17	3.06	2.58
Rank	1	2	3

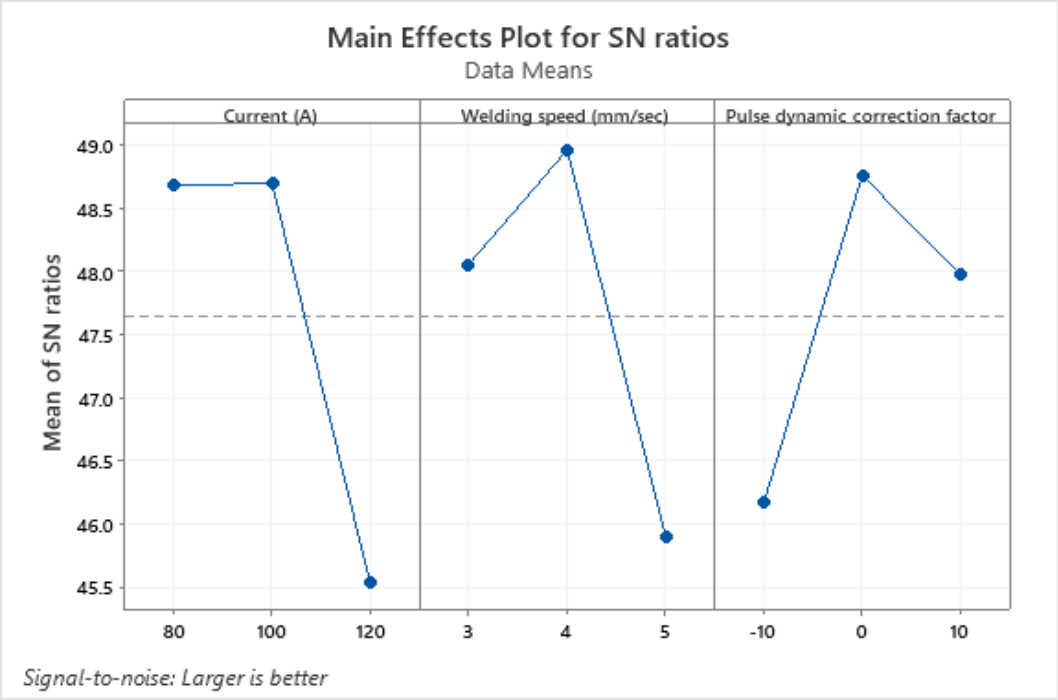

Figure 4.5: Mean S/N ratio graph for Yield Stress (YS)

Table 4.4: Response - Table for S/N for Maximum Percentage Elongation

Level	Current (A)	Welding Speed (mm/sec)	Pulse Dynamic Correction Factor (PDC)
1	34.83	34.76	35.20
2	34.72	35.29	35.70
3	35.53	35.03	34.18
Delta	0.81	0.53	1.52
Rank	2	3	1

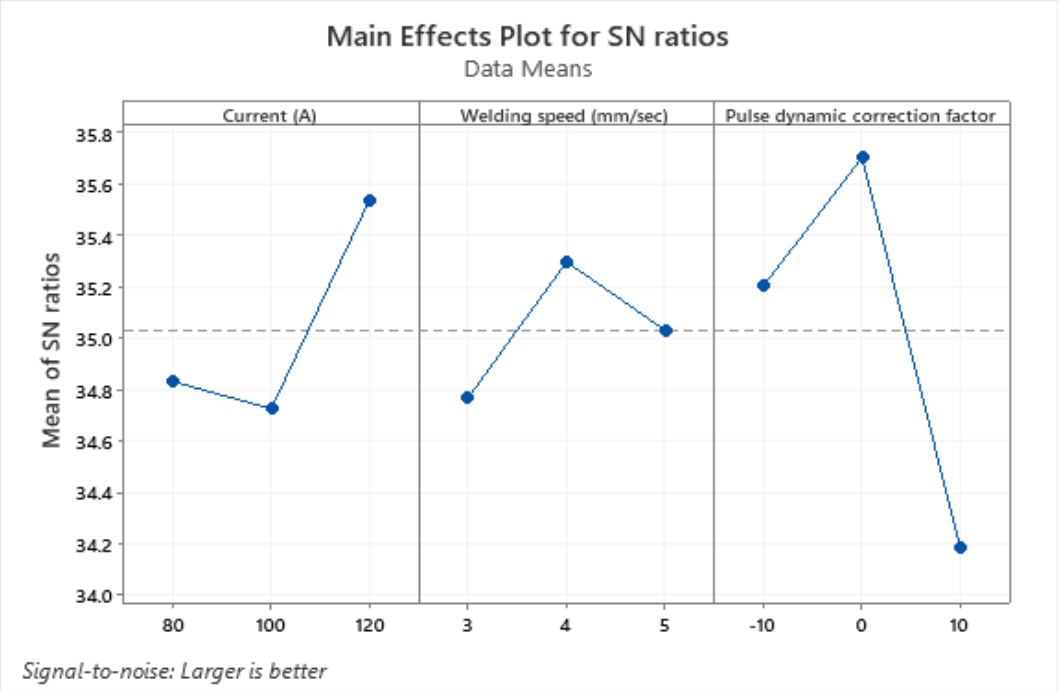

Figure 4.6: Mean S/N ratio graph for Percentage Elongation

Table 4.5. Response - Table for S/N Ratios for Maximum Yield strength (MPa), Ultimate tensile strength (MPa), Percentage elongation (%)

Level	Current (A)	Welding Speed (mm/sec)	Pulse Dynamic Correction Factor (PDC)
1	39.39	39.30	39.62
2	39.29	39.83	40.13
3	39.82	39.37	38.76
Delta	0.54	0.52	1.37
Rank	2	3	1

Figure 4.7: Mean S/N ratio graph for Yield strength (MPa), Ultimate tensile strength (MPa), Percentage elongation (%)

CHAPTER 5 ULTRASONIC ASSISTED CMT WELDING

5.1 INTRODUCTION

Ultrasound is always regarded as the cleanest and efficient source of energy with many other remarkable properties therefore it is immensely used in the field of manufacturing and processing. Ultrasonic-assisted arc welding is always the domain the of interest for many researchers over the past year. The idea is to influence the motion and solidification of the molten pool with the help of Ultrasonic vibration, so that mechanical and microstructural properties of the weld pool can be enhanced**.** [Zhao et al (2020)]

Ultrasonic assisted Shielded arc metal on SS 304 was studied by [Cui et al. (2007)]. The test result reported that the ultrasonic vibration can refine the grains of the work piece. Enhancement in joint strength, reduction in brittle intermetallic layer of Fe-Al, and refinement in grains was reported by [Dong et al. (2012)] while welding of aluminum alloy and steel using Ultrasonic assisted GTAW process. Due to Ultrasonic vibrations change of columnar grain to equiaxed grain around the weld pool was observed by [Chen et al. (2016)] during GTAW process aided with Ultrasonic vibration. Ultrasonic vibration can enhance the penetration of the weld, grain refinement, and improve the Ultimate tensile strength of the weld. [Wang et al. (2018)]

Increase in the mechanical properties was reported when the ultrasonic power increases, up to a certain limit, further increase in the ultrasonic power resulted in negative effect on the mechanical properties of the weld bead [Xu et al. (2014)] The difference in the mode of vibration influence the grain refinement which is mainly due difference in the convection which is influence by the vibration. This mainly depends on how the vibrations are applied, power of vibration. Clamping the work piece very tightly reduces the effect of vibration. [Wang et al. (2018)]. Solidification is affected by the Ultrasonic vibration [Tanghavi et al. (2009)]. Mechanical energy produced due to High vibration is converted into heat, hence the Ultrasonic vibration can assist in the fusion welding [Kumar et al. (2017)]**.** Ultrasonic Vibration inhibit the development of coarse grains [Fang et al. (2017)] Refinement of grains was observed by [Yuan et al. (2016)] with the help of Ultrasonic assisted welding of Mg alloys.

[Zhao et al. (2020)] examined the outcome of introducing Ultrasonic vibration on the molten weld pool while welding of 3mm thick Ti-6Al-4V alloy sheets by CMT plus pulse welding using the same material filler wire of diameter 1.2mm. The experimental was carried out at 5 m/min wire feed rate, 4mm/sec welding speed, at 12mm CTWD, and Argon (99.99 %) as the shielding gas. The test result concluded that the ultrasonic vibration when applied on the molten weld pool reduces the formation of the columnar grains near the fusion zone and increases the formation of more equiaxed grains. The phase was of the weld pool remained the same only the grains were refinement was observed along with increase in the tensile strength. [Fan et al. (2012)] examined effect of Ultrasonic vibration source assisted GMAW process mild steel base plate using ER70S-6 filler wire. The arc length increases with increase in the voltage for both GMAW and Ultrasonic assisted GMAW. However, the method of introducing the Ultrasonic Vibration to exploit the most under different welding condition is still to be determined.

[Watanabe et al. (2020)] observed that equiaxed grains were obtained by giving ultrasonic vibration to the molten weld pool. with the help of Ultrasonic vibration while welding of Aluminum alloys high refinement in grains was observed [Atamanenko et al. (2010)]. [Tian et al. (2018)] welded AA6061 of 4 mm thickness by Ultrasonic assisted CMT welding process using ER 4043 as filler wire of diameter 1.2 mm and 99.9% Argon as shielding gas. The vibration frequency given was 3mm and 35micron. The experimental results disclosed that penetration and weld reinforcement was increased and density of pores was decreased. The refined grain size obtained was in the range of 50nm to 500nm. [Zhao et al. (2020)] welded magnesium alloy AZ40 and DP780 galvanized stainless steel using Ultrasonic assisted TIG welding and reported an enhancement by 8% in ultimate tensile strength of the weld bead.

However, the method of introducing the Ultrasonic Vibration to exploit the most under different welding condition is still to be determined. Very less research is done on Ultrasonic Assisted CMT welding process. In this project ultrasonic assisted CMT welding was carried out on SS 202 samples of thickness 1.58mm and results were compared with the data obtained from normal CMT process. The stress strain graph was plotted for the welded

samples obtained by both the process at the same process parameter to compare the exact nature of the samples under stress.

5.2 EXPERIMENTAL PROCEDURE

5.2.1 MATERIALS AND METHOD

The ultrasonic assisted CMT was carried out on SS 202 samples of dimensions 100mm × 60mm × 1.58mm using an Ultrasonic probe of 20 KHz frequency. The experimental set up is shown in Figure 5.1. Similar SS 308 filler wire of diameter 1.2mm and shielding gas with 98 % argon and 2 % CO_2 composition was used for conducting the experiment as it was used for conducting CMT welding as mentioned above in chapter 3. The contact tip to work distance and gas flow rate was kept constant at 10mm and 15 L/min respectively. The clamping was done in such a way that the vibration can be felt on the base metal and the probe was set up in manner that direct vibration can be applied on the base plate.

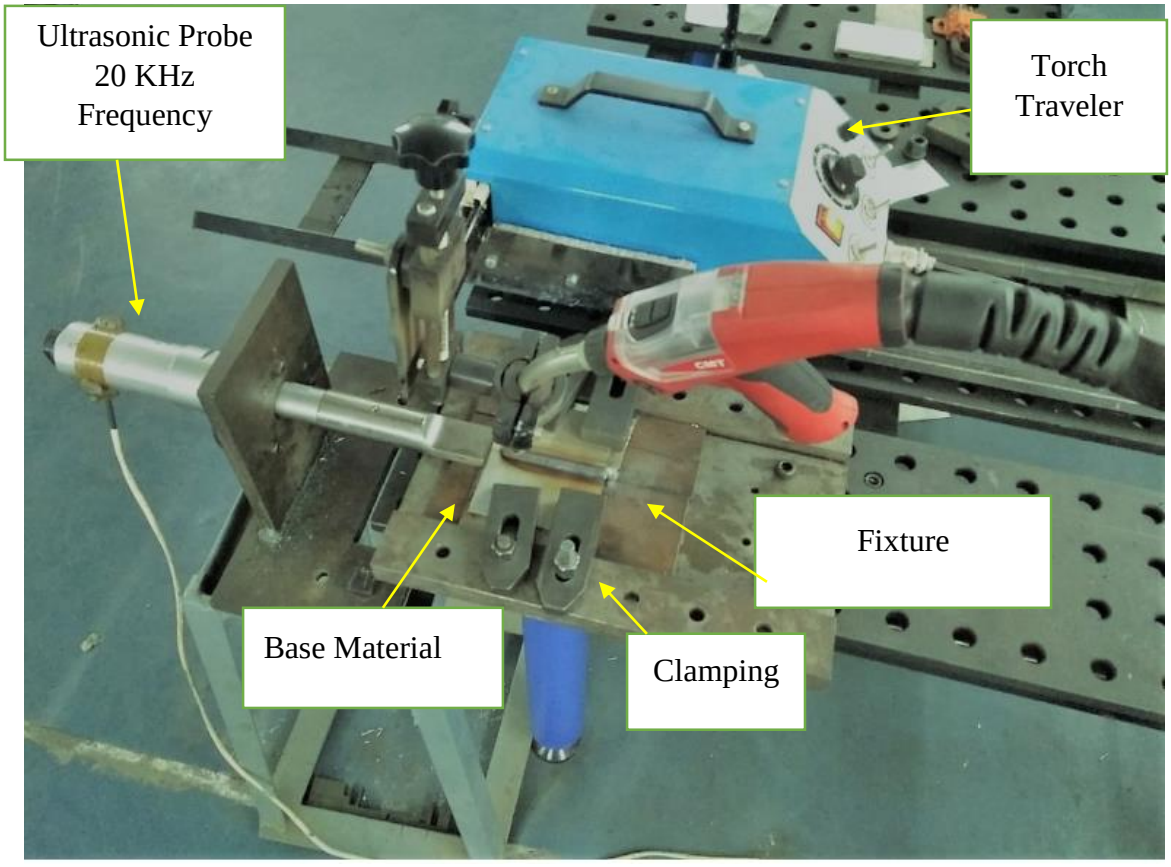

Figure 5.1 Experimental Set for Ultrasonic Assisted Cold Metal Transfer Welding

5.2.2 PROCESS PARAMETER

The experiments were carried out 3 different process parameter wherein the 3 different values of current were 80A, 100A and 120A, welding speed were 3mm/sec, 4mm/sec and 5mm/sec and Pulse dynamic factor were -10, 0, +10. Again Taguchi L9 orthogonal array was used for finding the best parametric combination to carry out the welding. The amplitude of vibration was kept constant at 99 microns for all the result which was given by Ultrasonic probe. Table 5.1 shows the value of process parameters for the 4 samples. All the welded samples are shown in figure 5.2. The welded samples at different process parameters are individually shown in figure 5.3, figure 5.4, figure 5.5, figure 5.6 respectively. Table 5.2, Table 5.3, Table 5.4 and Table 5.5 shows the process parameter value for the welded samples. The welded samples are labelled by UCMT for Ultrasonic assisted CMT of CMT welding with vibrations.

Table 5.1 Process Parameter Matrix for Ultrasonic assisted CMT (UCMT) welding of SS 202 sample of thickness 1.58 mm

Sample No.	Current (A)	Welding Speed (mm/sec)	Pulse Dynamic Correction Factor
Sample 1	120 A	3 mm/sec	+10
Sample 2	100 A	4 mm/sec	+10
Sample 3	80 A	3 mm/sec	-10
Sample 4	100 A	3 mm/sec	0

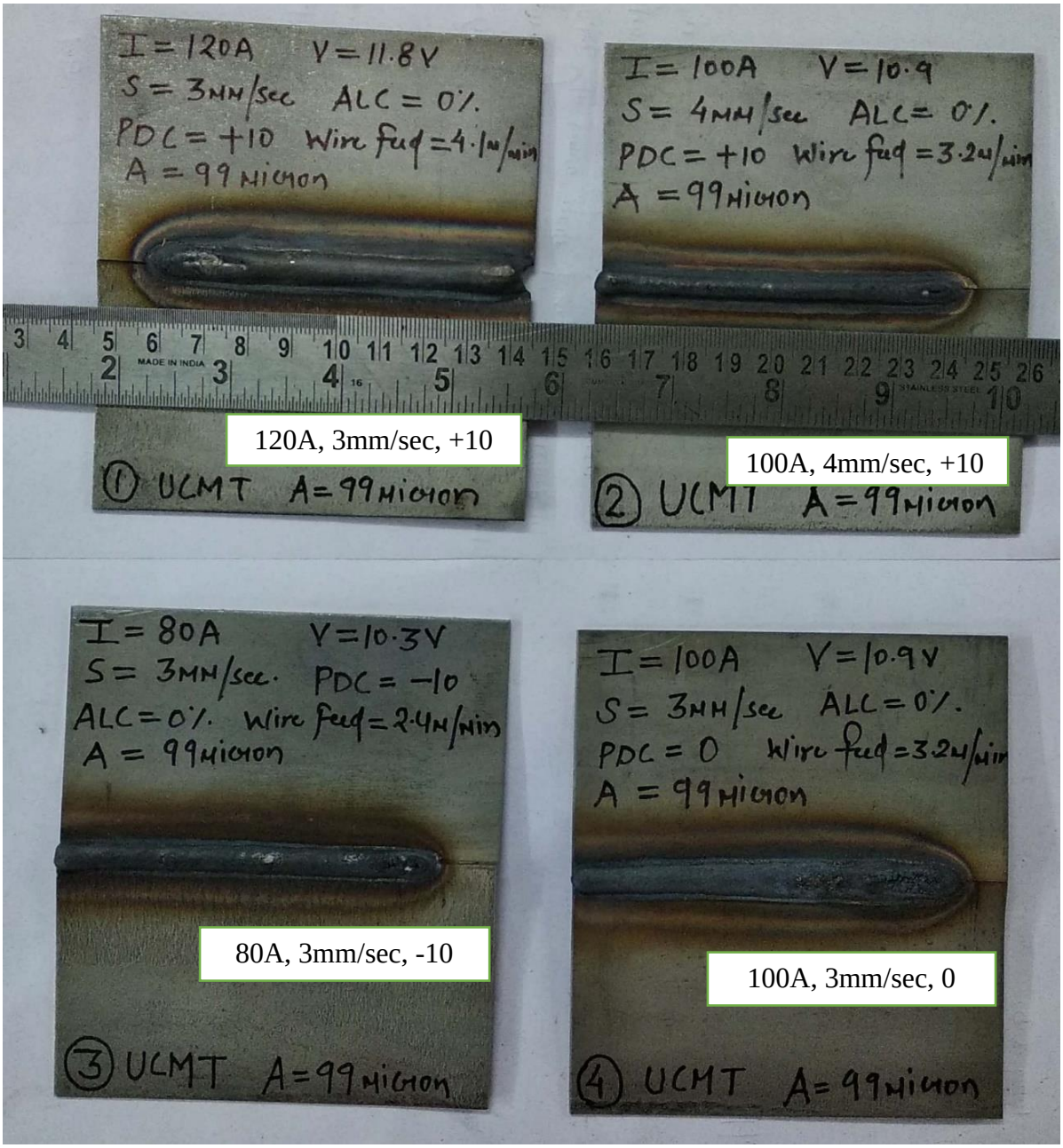

Figure 5.2: Ultrasonic assisted CMT (UCMT) welded SS 202 Samples of thickness 1.58 mm at different process parameters

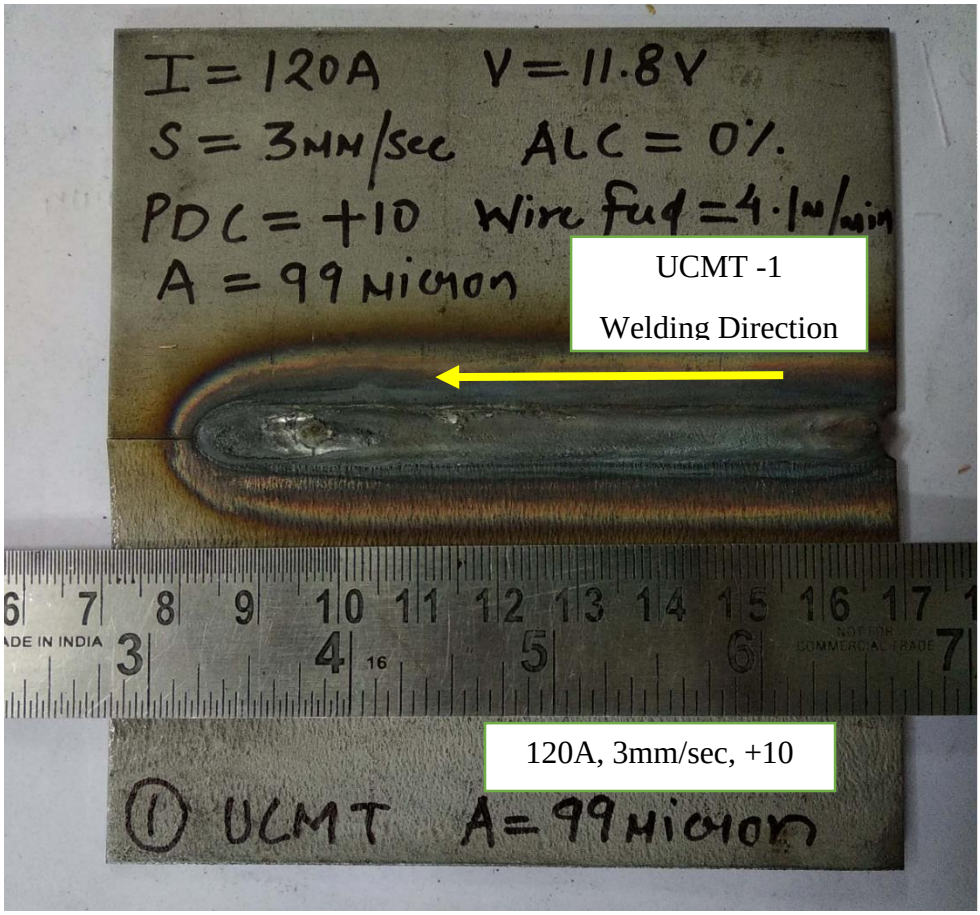

Figure 5.3: Image of UCMT welded SS 202 of thickness 1.58 mm at Current 120A, Welding Speed 3mm/sec, and Pulse dynamic correction Factor +10

Table 5.2: Process Parameter Matrix for UCMT welded sample 1

Process Parameter	Value
Current (A)	120 A
Welding Sped (mm/sec)	3 mm/sec
Pulse Dynamic Correction Factor	+10
Voltage (V)	11.8 V
Wire feed rate (m/min)	4.1 m/min
Arc length Correction Factor (%)	0 %
Contact Tip to work distance (mm)	10 mm
Amplitude (micron)	99

Figure 5.4: Image of UCMT welded SS 202 of thickness 1.58 mm at Current 100A, Welding Speed 4mm/sec, and Pulse dynamic correction Factor +10

Table 5.3: Process Parameter Matrix for UCMT welded sample 2

Process Parameter	Value
Current (A)	100 A
Welding Sped (mm/sec)	4 mm/sec
Pulse Dynamic Correction Factor	+10
Voltage (V)	10.9 V
Wire feed rate (m/min)	3.2 m/min
Arc length Correction Factor (%)	0 %
Contact Tip to work distance (mm)	10 mm
Amplitude (micron)	99 micron

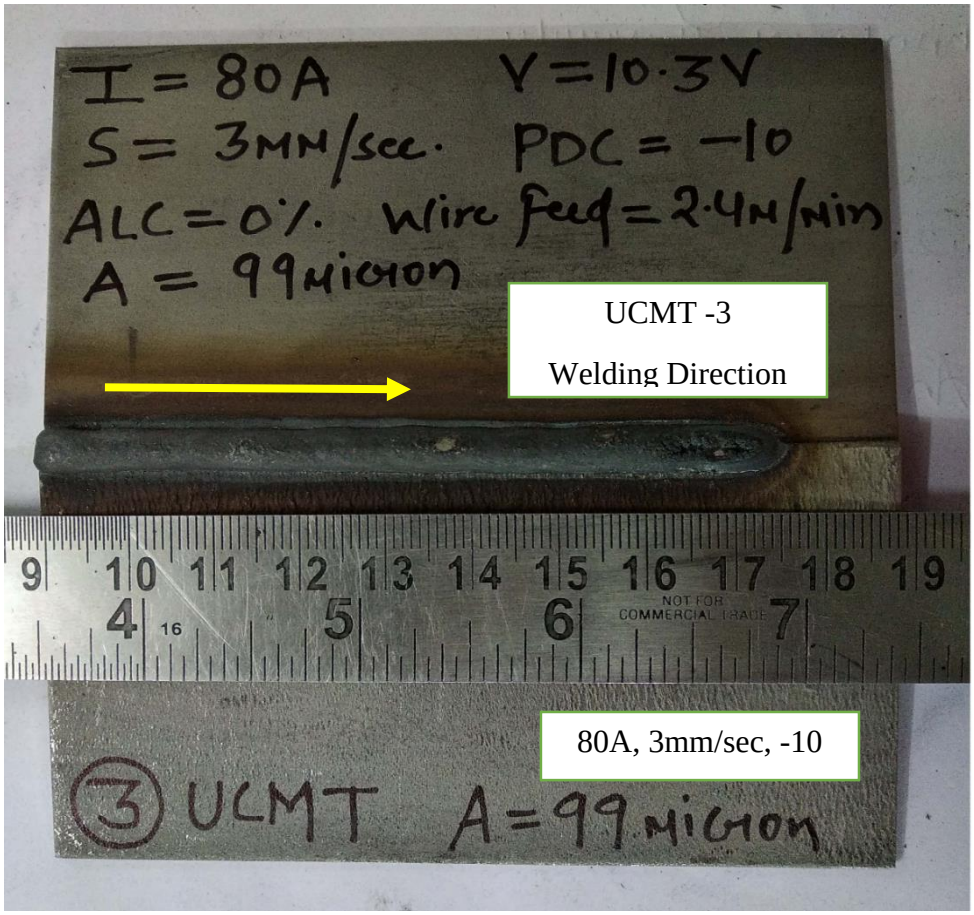

Figure 5.5: Image of UCMT welded SS 202 of thickness 1.58 mm at Current 80A, Welding Speed 3mm/sec, and Pulse dynamic correction Factor -10

Table 5.4: Process Parameter Matrix for UCMT welded sample 3

Process Parameter	Value
Current (A)	80 A
Welding Sped (mm/sec)	3 mm/sec
Pulse Dynamic Correction Factor	-10
Voltage (V)	10.3 V
Wire feed rate (m/min)	2.4 m/min
Arc length Correction Factor (%)	0 %
Contact Tip to work distance (mm)	10 mm
Amplitude (micron)	99 micron

Figure 5.6: Image of UCMT welded SS 202 of thickness 1.58 mm at Current 100A, Welding Speed 3mm/sec, and Pulse dynamic correction Factor 0

Table 5.5: Process Parameter Matrix for UCMT welded sample 4

Process Parameter	Value
Current (A)	100 A
Welding Sped (mm/sec)	3 mm/sec
Pulse Dynamic Correction Factor	0
Voltage (V)	10.9 V
Wire feed rate (m/min)	3.2 m/min
Arc length Correction Factor (%)	0 %
Contact Tip to work distance (mm)	10 mm
Amplitude (micron)	99 micron

5.3 TENSILE TESTING

The test specimens were cut from the welded samples as per ASTM E8 standards using wire cut EDM process as shown in figure 5.7. The tensile testing was done using TINIUS OLSEN UTM H50KS of 50 KN machine. The value of Ultimate tensile strength, Yield strength and Percentage elongation was obtained using the testing. Table 5.6 shows the responses obtained after Tensile testing.

Figure 5.7: Test specimens for tensile testing taken from UCMT welded samples

Table 5.6: Process parameter and Response table for Ultrasonic assisted CMT (UCMT) welding of SS 202 sample of thickness 1.58 mm

Welding Process Parameter			Responses		
Welding Current (A)	Welding Speed (mm/sec)	Pulse Dynamic Correction Factor (PDC)	Ultimate Tensile Strength (MPa)	Yield Strength (MPa)	Percentage Elongation (%)
120 A	3 mm/sec	+10	768 MPa	340 MPa	52.4 %
100 A	4 mm/sec	+10	618 MPa	352 MPa	38.0 %
80 A	3 mm/sec	-10	737 Mpa	329 MPa	48.4 %
100 A	3 mm/sec	0	801 Mpa	330 MPa	58.4 %

5.4 RESULTS AND DISCUSSION

From experimental data as shown is Table 5.6 the highest value of Ultimate Tensile Strength of 801 Mpa was obtained for the Ultrasonic assisted CMT welded samples was at 100A current, 3mm/sec welding speed and 0 pulse dynamic correction factor. [Watanabe et al. (2010)] reported about 30% percentage elongation for GTAW welded steels sheets of 1mm thickness with Ultrasonic vibrations. In this research work. 58.4 % of percentage elongation was the most superior value out of all the samples which was recorded at 100A current, 3mm/sec welding speed and 0 pulse dynamic correction factor. For the Yield Strength value superior value out of all the samples was obtained at 100A current, 4mm/sec welding speed and +10 Pulse dynamic correction factor. The penetration of the weld bead is increased by Ultrasonic vibration [Dai et al. (2003)] due to Ultrasonic vibrations effect. Figure 5.8 shows comparison of specimen cut from the CMT welded samples and UCMT welded samples for the tensile Testing. In this research work also deeper penetration of the weld can be visualized. Enhancement of Mechanical properties reported by [Zhao et al. (2020)] using Ultrasonic assisted CMT welding. Table 5.7 and Table 5.8 shows comparison of Ultimate Tensile Stress and Percentage Elongation Value between CMT welded and corresponding UCMT welded samples at same Process Parameter respectively. At current 120A, welding speed 3mm/sec and +10 Pulse dynamic correction factor superior value for Ultimate Tensile strength and Percentage Elongation that was reported for CMT welded sample was 763 MPa and 50.4% respectively. In comparison to this superior value for these two properties that was reported by UCMT welded samples at the same process parameter were 768 Mpa and 52.5% respectively. For Yield Strength almost all the samples showed higher value for UCMT welded samples in comparison to CMT welded samples as shown in Table 5.9. At 100A current, 4mm/sec welding speed and -10 Pulse dynamic correction factor superior value of Yield strength with vibration was 352 MPa and 279 Mpa without vibration. An increase of 37.9 % in yield strength was obtained at current 80A, Welding speed 3mm/sec and Pulse dynamic factor -10. Comparison of Yield Strength Value between the samples welded by CMT with and without vibration is shown in Figure 5.13. Stress strain curve for the CMT welded and UCMT welded samples at the same process parameter is shown in Figure 5.9, Figure 5.10, Figure 5.11 and Figure 5.12. The yield strength is the properties of material which denotes their load bearing capacity without any permanent deformation. Till

Yield point material is in their elastic limit and after yield point permanent deformation starts and material goes to plastic region. Since CMT welded samples with Ultrasonic vibration is showing higher yield point value hence, better load bearing capacity before permanent deformation occurs in the material in comparison to CMT welded samples without Ultrasonic vibrations.

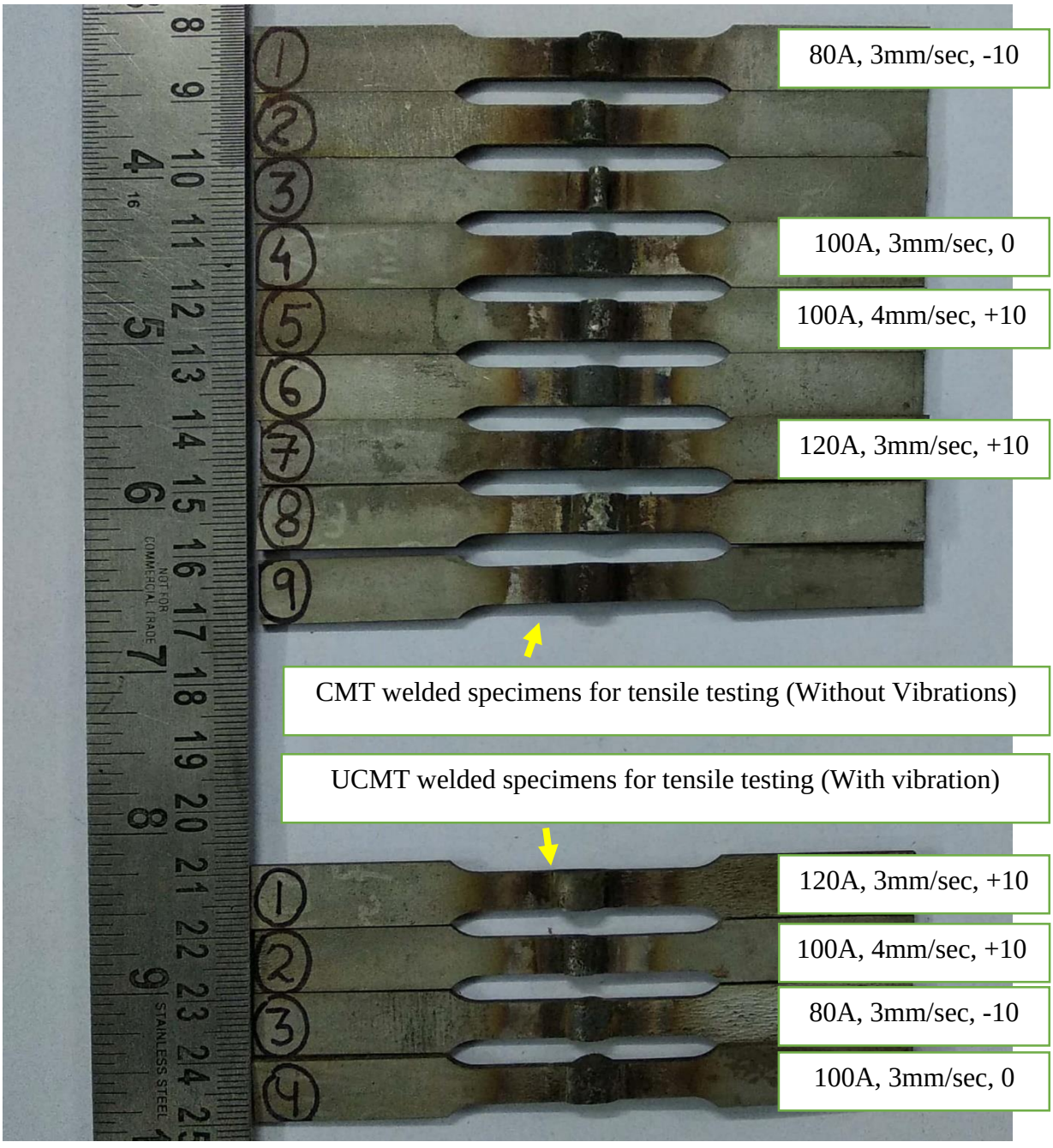

FIGURE 5.8: Test specimens cut for Tensile Testing from CMT welded (without vibrations) Samples and UCMT welded Samples (with vibrations)

Table 5.7: Comparison of Ultimate Tensile Stress Value between CMT welded and corresponding UCMT welded SS 202 Samples at same Process Parameter

Current (A)	Welding Speed (mm/sec)	Pulse Dynamic Correction Factor	Ultimate Tensile Stress (Mpa) (CMT)	Ultimate Tensile Stress (Mpa) (UCMT)
80 A	3 mm/sec	-10	807 Mpa	737 Mpa
100 A	3 mm/sec	0	860 Mpa	801 Mpa
100 A	4 mm/sec	+10	742 Mpa	618 Mpa
120 A	3 mm/sec	+10	763 Mpa	768 Mpa

Table 5.8: Comparison of Percentage Elongation Value between CMT welded and corresponding UCMT welded SS 202 Samples at same Process Parameter

Current (A)	Welding Speed (mm/sec)	Pulse Dynamic Correction Factor	Percentage Elongation (%) (CMT)	Percentage Elongation (%) (UCMT)
80 A	3 mm/sec	-10	54.4 %	48.8%
100 A	3 mm/sec	0	59.8 %	58.3%
100 A	4 mm/sec	+10	50.8 %	38.1%
120 A	3 mm/sec	+10	50.4 %	52.5%

Table 5.9. Comparison of Yield Stress Value between CMT welded and corresponding UCMT welded SS 202 Samples at same Process Parameter

Current (A)	Welding Speed (mm/sec)	Pulse Dynamic Correction Factor	Yield Stress (Mpa) (CMT)	Yield Stress (Mpa) (UCMT)
80 A	3 mm/sec	-10	204 Mpa	329 Mpa
100 A	3 mm/sec	0	365 Mpa	330 Mpa
100 A	4 mm/sec	+10	279 Mpa	352 Mpa
120 A	3 mm/sec	+10	217 Mpa	340 Mpa

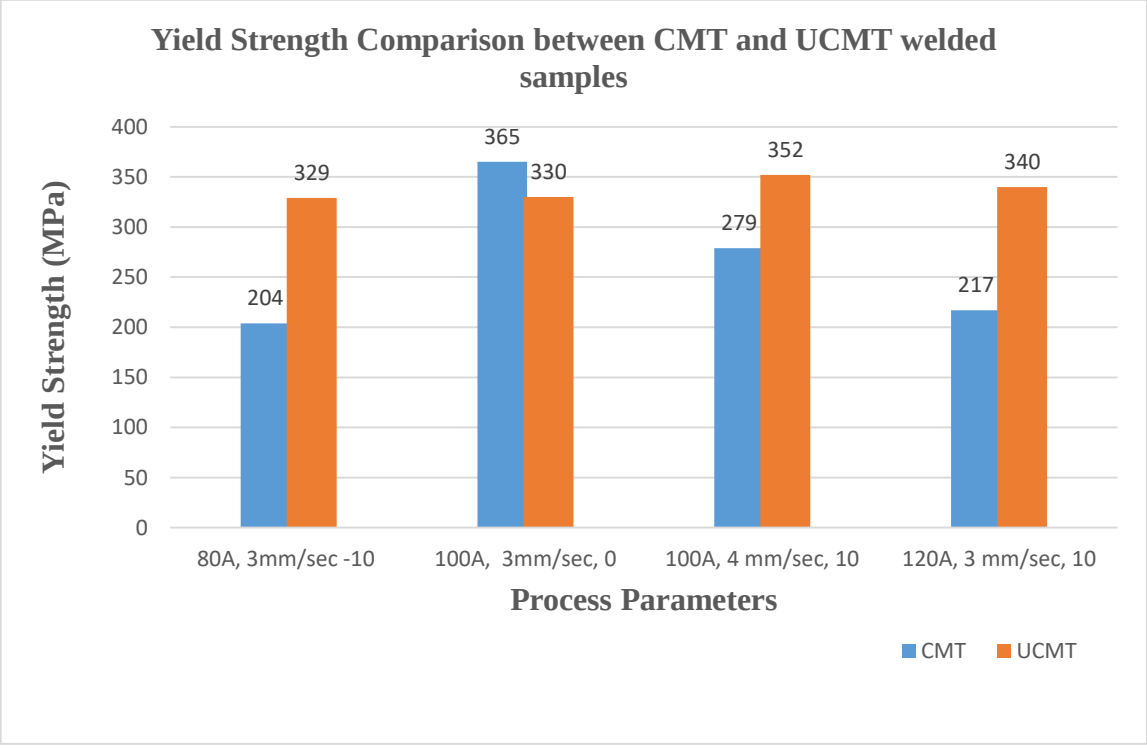

Figure 5.9: Comparison of Yield Strength Value between CMT welded and UCMT welded Specimen

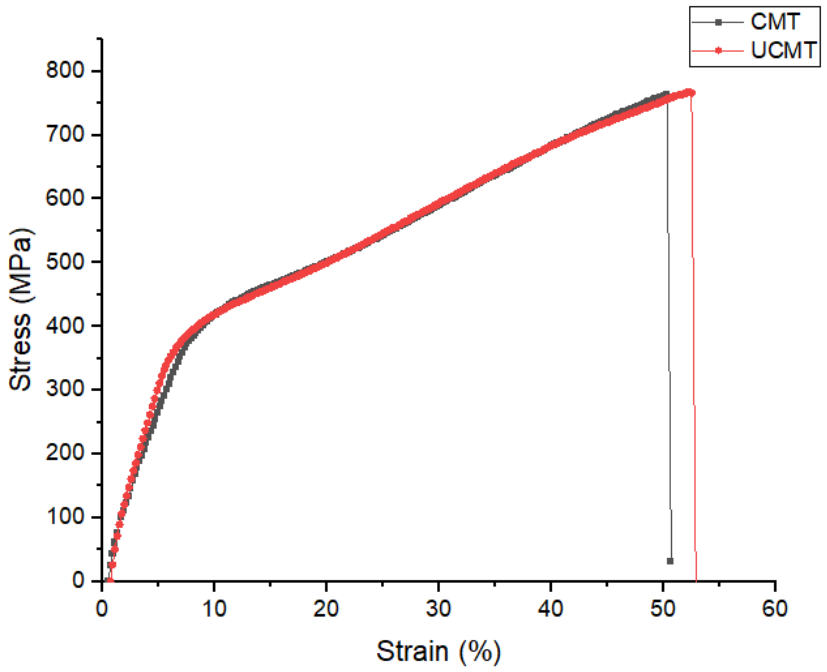

Figure 5.10: Stress- Strain curve for CMT welded sample and UCMT welded Sample at Current - 120A, Welding Speed – 3mm/sec, Pulse dynamic correction factor - +10

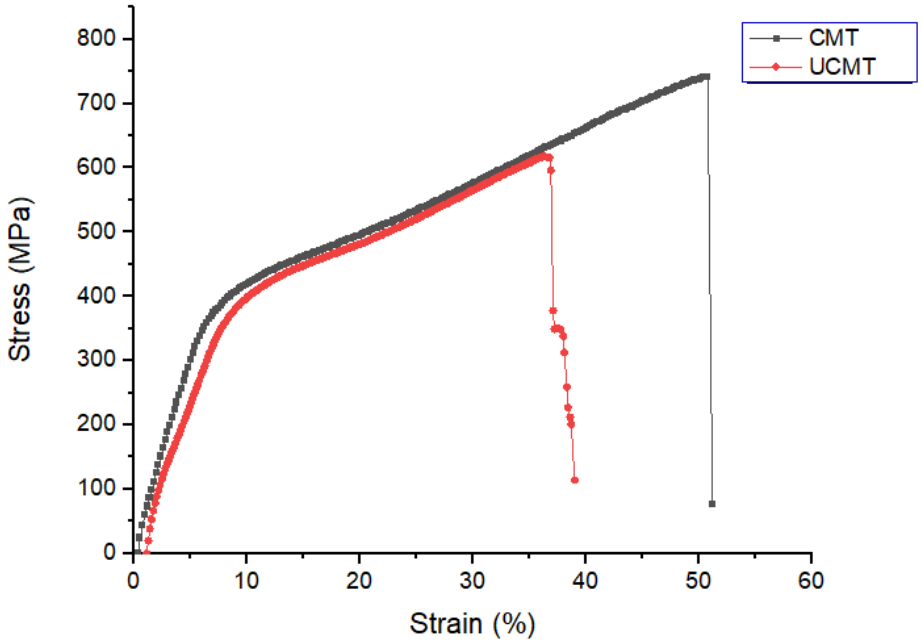

Figure 5.11: Stress- Strain curve for CMT welded Sample and UCMT welded Sample at Current -100A, Welding Speed – 4mm/sec, Pulse dynamic correction factor - +10

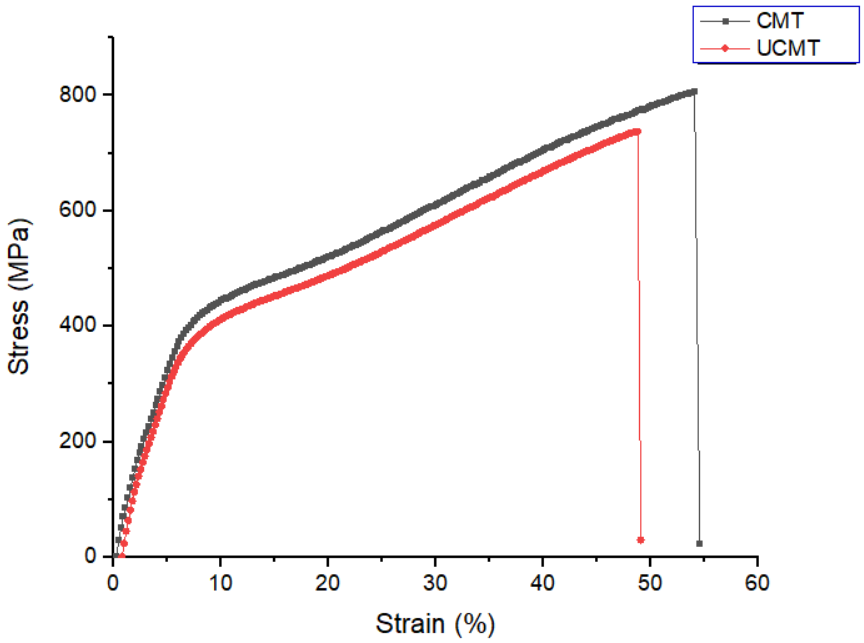

Figure 5.12: Stress- Strain curve for CMT welded sample and UCMT welded Sample at Current - 80A, Welding Speed – 3mm/sec, Pulse dynamic correction factor - -10

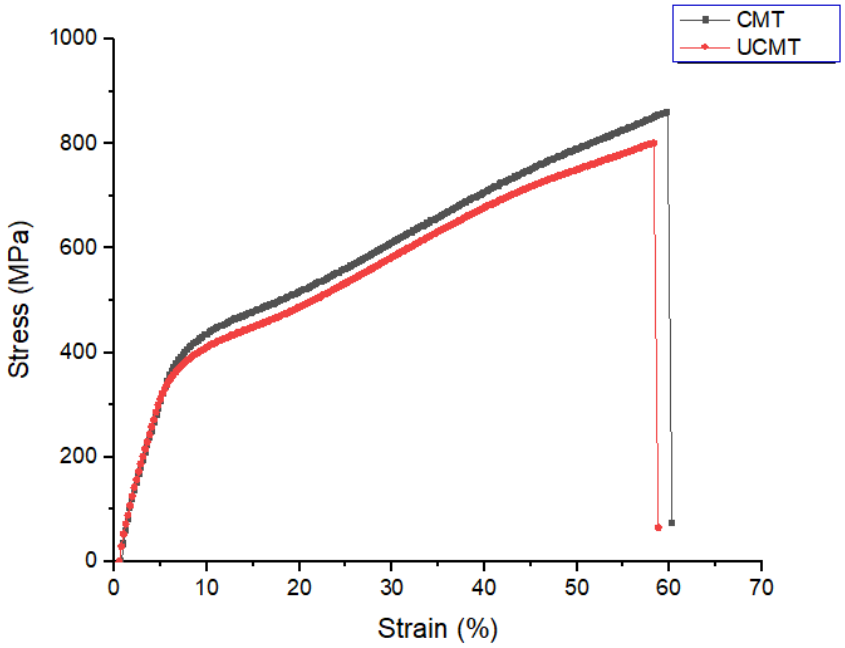

Figure 5.13: Stress- Strain curve for CMT welded Sample and UCMT welded Sample at Current - 100A, Welding Speed – 3mm/sec, Pulse dynamic correction factor – 0

CHAPTER 6 CONCLUSIONS

In this research work welding of SS202 austenitic stainless steel samples was successfully welded by CMT welding with and without Ultrasonic vibrations. The experiments were done at optimized process parameters on the basis of Taguchi's L9 design of array using Minitab 19 software and the test results were validated and optimized by Taguchi's S/N ratio higher the better criteria. Following conclusions are drawn from the results obtained from this research work.

1) Weld bead of SS202 sheets of thickness 1.58 mm when welded by CMT Welding process showed excellent weldability and satisfactory Yield Strength, Ultimate tensile strength, and Percentage elongation.
2) From experimental results maximum values of Yield Strength, Ultimate Tensile Strength, and Percentage Elongation obtained were 379 MPa, 871 MPa, and 65.9 % respectively.
3) From Taguchi S/N ratio larger the better criteria, most optimum combination of process parameter for obtaining maximum:
   (a) Ultimate Tensile Strength value is C3S1P2 that is at 120A current, 3 mm/sec welding speed and 0 Pulse dynamic correction factor.
   (b) Yield Strength value is C2S2P2 that is at 100A current, 4 mm/sec welding speed and 0 Pulse dynamic correction factor.
   (c) Percentage Elongation value is C3S2P2 that is at 120A current, 4 mm/sec speed and 0 Pulse dynamic correction factor.
4) From Taguchi S/N ratio higher the better criteria, most optimum combination of process parameter for obtaining maximum Yield Strength (YS), Ultimate tensile strength (UTS), and Percentage Elongation simultaneously for a single sample is C3S2P2 that is at 120A current, 4 mm/sec speed and 0 Pulse dynamic correction factor.
5) At 0 Pulse dynamic correction factor most significant result were reported by Taguchi S/N ratio larger the better criteria, as discussed above in conclusion 3 and 4, which indicates both fast and slow rate of droplet detachment at constant energy level affects the weld bead properties.
6) Ultrasonic vibration assisted CMT welding process reported improvement in mechanical properties especially in Yield strength value. An increase of 37.9 % in Yield Strength

value was obtained for the sample welded with Ultrasonic vibration in comparison to sample welded without Ultrasonic vibration at the same process parameter.

7) Better load bearing capacity before plastic deformation was shown by samples welded by CMT assisted Ultrasonic vibration in comparison to CMT welded sample without ultrasonic vibrations.

REFERENCES

Ahsan, Md RU, Y. R. Kim, R. Ashiri, Y. J. Cho, C. Jeong, and Y. D. Park. "Cold metal transfer (CMT) GMAW of zinc-coated steel." *Welding Journal* 95, no. 4 (2016): 120-132.

Alipooramirabad, Houman, Anna Paradowska, Reza Ghomashchi, and Mark Reid. "Investigating the effects of welding process on residual stresses, microstructure and mechanical properties in HSLA steel welds." *Journal of Manufacturing Processes* 28 (2017): 70-81.

Atamanenko, T. V., D. G. Eskin, L. Zhang, and L. Katgerman. "Criteria of grain refinement induced by ultrasonic melt treatment of aluminum alloys containing Zr and Ti." *Metallurgical and Materials Transactions A* 41, no. 8 (2010): 2056-2066.

Babu, S., S. K. Panigrahi, GD Janaki Ram, P. V. Venkitakrishnan, and R. Suresh Kumar. "Cold metal transfer welding of aluminium alloy AA 2219 to austenitic stainless steel AISI 321." *Journal of Materials Processing Technology* 266 (2019): 155-164.

Baddoo, N. R. "Stainless steel in construction: A review of research, applications, challenges and opportunities." *Journal of constructional steel research* 64, no. 11 (2008): 1199-1206.

Bharwal, Sahil, and Charit Vyas. "Weldability issue of AISI 202 SS (stainless steel) grade with GTAW process compared to AISI 304 SS grade." *Int. J. Adv. Mech. Eng* 4 (2014): 695-700.

Biswas, Amit Ratan, Sadananda Chakraborty, Partha Sarathi Ghosh, and Dipankar Bose. "Study Of Parametric Effects On Mechanical Properties Of Stainless Steel (AISI 304) And Medium Carbon Steel (45C8) Welded Joint Using GMAW." *Materials Today: Proceedings* 5, no. 5 (2018): 12384-12393.

Bunaziv, Ivan, Odd M. Akselsen, Jan Frostevarg, and Alexander FH Kaplan. "Laser-arc hybrid welding of thick HSLA steel." *Journal of Materials Processing Technology* 259 (2018): 75-87.

Caballero, Armando, Jialuo Ding, Supriyo Ganguly, and Stewart Williams. "Wire+ Arc Additive Manufacture of 17-4 PH stainless steel: Effect of different processing conditions on

microstructure, hardness, and tensile strength." *Journal of Materials Processing Technology* 268 (2019): 54-62.

Cao, R., J. H. Sun, J. H. Chen, and Peichung Wang. "Weldability of CMT joining of AA6061-T6 to boron steels with various coatings." *Weld. J* 93, no. 6 (2014): 193s-204s.

Cao, R., Q. Huang, J. H. Chen, and Pei-Chung Wang. "Cold metal transfer spot plug welding of AA6061-T6-to-galvanized steel for automotive applications." *Journal of alloys and compounds* 585 (2014): 622-632.

Cao, X., P. Wanjara, J. Huang, C. Munro, and A. Nolting. "Hybrid fiber laser–Arc welding of thick section high strength low alloy steel." *Materials & Design* 32, no. 6 (2011): 3399-3413.

Chan, Kai Wang, and Sie Chin Tjong. "Effect of secondary phase precipitation on the corrosion behavior of duplex stainless steels." *Materials* 7, no. 7 (2014): 5268-5304.

Chen, Maoai, Dong Zhang, and Chuansong Wu. "Current waveform effects on CMT welding of mild steel." *Journal of Materials Processing Technology* 243 (2017): 395-404.

Chen, Qi-Hao, San-Bao Lin, Chun-Li Yang, Cheng-Lei Fan, and Hong-Liang Ge. "Effect of ultrasound on heterogeneous nucleation in TIG welding of Al–Li alloy." *Acta Metallurgica Sinica (English Letters)* 29, no. 12 (2016): 1081-1088.

Chen, Shuhai, Siqi Li, Yan Li, Jihua Huang, Shujun Chen, and Jian Yang. "Butt welding-brazing of steel to aluminum by hybrid laser-CMT." *Journal of Materials Processing Technology* 272 (2019): 163-169.

Coelho, R. S., A. Kostka, H. Pinto, S. Riekehr, M. Kocak, and A. R. Pyzalla. "Microstructure and mechanical properties of magnesium alloy AZ31B laser beam welds." *Materials Science and Engineering: A* 485, no. 1-2 (2008): 20-30.

Cole, G. S., and A. M. Sherman. "Light weight materials for automotive applications." *Materials characterization* 35, no. 1 (1995): 3-9.

Cong, Baoqiang, Ruijie Ouyang, Bojin Qi, and Jialuo Ding. "Influence of cold metal transfer process and its heat input on weld bead geometry and porosity of aluminum-copper alloy welds." *Rare Metal Materials and Engineering* 45, no. 3 (2016): 606-611.

Cui, Yan, Cailu Xu, and Qingyou Han. "Microstructure improvement in weld metal using ultrasonic vibrations." *Advanced Engineering Materials* 9, no. 3 (2007): 161-163.

Czyryca, Ernest J., Richard E. Link, Richard J. Wong, Denise A. Aylor, Thomas W. Montem, and John P. Gudas. "Development and certification of HSLA-100 steel for naval ship construction." *Naval engineers journal* 102, no. 3 (1990): 63-82.

Dai, Wen-Long. "Effects of high-intensity ultrasonic-wave emission on the weldability of aluminum alloy 7075-T6." *Materials Letters* 57, no. 16-17 (2003): 2447-2454.

Devakumar, D., and D. B. Jabaraj. "Research on gas tungsten arc welding of stainless steel–an overview." *International Journal of Scientific & Engineering Research* 5, no. 1 (2014): 1612-1618.

Dharmik, Bhushan Y., and Nitin Kumar Lautre. "Performance Assessment of CMT over GTA welding on stacked thin sheets of CRNGO Electrical steel." *Materials Letters* (2020): 127901.

Dhobale, A. L., and H. K. Mishra. "Review on effect of heat input on tensile strength of butt weld joint using mig welding." *International Journal of Innovations in Engineering Research and Technology* 2, no. 9 (2015): 1-13.

Dirisu, Philip, Supriyo Ganguly, Ali Mehmanparast, Filomeno Martina, and Stewart Williams. "Analysis of fracture toughness properties of wire+ arc additive manufactured high strength low alloy structural steel components." *Materials Science and Engineering: A* 765 (2019): 138285.

Dong, Honggang, Liqun Yang, Chuang Dong, and Sindo Kou. "Improving arc joining of Al to steel and Al to stainless steel." *Materials Science and Engineering: A* 534 (2012): 424-435.

Du Toit, Madeleine, and Herman G. Steyn. "Comparing the formability of AISI 304 and AISI 202 stainless steels." *Journal of materials engineering and performance* 21, no. 7 (2012): 1491-1495.

Dutra, Jair Carlos, Régis Henrique Gonçalves e Silva, Bruna Martinello Savi, Cleber Marques, and Orestes Estevam Alarcon. "Metallurgical characterization of the 5083H116 aluminum alloy welded with the cold metal transfer process and two different wire-electrodes (5183 and 5087)." *Welding in the World* 59, no. 6 (2015): 797-807.

Elrefaey, A. "Effectiveness of cold metal transfer process for welding 7075 aluminium alloys." *Science and Technology of Welding and Joining* 20, no. 4 (2015): 280-285.

Fan, Y. Y., C. L. Yang, S. B. Lin, C. L. Fan, and W. G. Liu. "Ultrasonic wave assisted GMAW." *Weld J* 91, no. 3 (2012): 91s-99s.

Fang, Xiaogang, Shusen Wu, Shulin Lü, Jing Wang, and Xiong Yang. "Microstructure evolution and mechanical properties of quasicrystal-reinforced Mg-Zn-Y alloy subjected to ultrasonic vibration." *Materials Science and Engineering: A* 679 (2017): 372-378.

Faridmehr, Iman, M. Hanim Osman, A. Bin Adnan, A. Farokhi Nejad, Reza Hodjati, and Mohammadamin Azimi. "Correlation between engineering stress-strain and true stress-strain curve." *American Journal of Civil Engineering and Architecture* 2, no. 1 (2014): 53-59.

Feng, Ji-Cai, Ya-Rong Wang, and Zhong-Dian Zhang. "Status and expectation of research on welding of magnesium alloy." *Chinese Journal of Nonferrous Metals* 15, no. 2 (2005): 165-178.

Frostevarg, Jan, Alexander FH Kaplan, and Javier Lamas. "Comparison of CMT with other arc modes for laser-arc hybrid welding of steel." *Welding in the World* 58, no. 5 (2014): 649-660.

Gautam, Kamal Kant, Onkar Singh Bhatia, and R. P. Singh. "Analysis of Weldability AISI 202 SS (Stainless Steel)." *International Journal of Emerging Technologies in Engineering Research* 6 (2018): 31-34.

Ge, Jinguo, Jian Lin, Yongping Lei, and Hanguang Fu. "Location-related thermal history, microstructure, and mechanical properties of arc additively manufactured 2Cr13 steel using cold metal transfer welding." *Materials Science and Engineering: A* 715 (2018): 144-153.

Ghosh, Nabendu, Pradip Kumar Pal, and Goutam Nandi. "Parametric optimization of MIG welding on 316L austenitic stainless steel by Grey-Based Taguchi method." *Procedia Technology* 25 (2016): 1038-1048.

Ghosh, Nabendu, Pradip Kumar Pal, Goutam Nandi, and Ramesh Rudrapati. "Parametric optimization of gas metal arc welding process by PCA based Taguchi method on austenitic stainless steel AISI 316L." *Materials Today: Proceedings* 5, no. 1 (2018): 1620-1625.

Gungor, Beytullah, Erdinc Kaluc, Emel Taban, and S. I. K. Aydin. "Mechanical and microstructural properties of robotic Cold Metal Transfer (CMT) welded 5083-H111 and 6082-T651 aluminum alloys." *Materials & Design (1980-2015)* 54 (2014): 207-211.

Guojin, Li, Zhang Peilei, Wu Xi, Nie Yunpeng, Yu Zhishui, Yan Hua, and Lu Qinghua. "Gap bridging of 6061 aluminum alloy joints welded by variable-polarity cold metal transfer." *Journal of Materials Processing Technology* 255 (2018): 927-935.

Ishimaru, Eiichiro, Hiroshi Hamasaki, and Fusahito Yoshida. "Deformation-induced martensitic transformation and workhardening of type 304 stainless steel sheet during draw-bending." *Procedia Engineering* 81 (2014): 921-926.

Juang, S. C., and Y. S. Tarng. "Process parameter selection for optimizing the weld pool geometry in the tungsten inert gas welding of stainless steel." *Journal of materials processing technology* 122, no. 1 (2002): 33-37.

Jurica, Maja, Z. Kozuh, I. Garasic, and M. Busic. "Optimization of the A-TIG welding for stainless steels." In *IOP Conf Ser: Mater Sci Eng*, vol. 329, no. 1, pp. 1-9. 2018.

Kadoi, Kota, Aoi Murakami, Kenji Shinozaki, Motomichi Yamamoto, and Hideo Matsumura. "Crack repair welding by CMT brazing using low melting point filler wire for long-term used steam turbine cases of Cr-Mo-V cast steels." *Materials Science and Engineering: A* 666 (2016): 11-18.

Kannan, A. Rajesh, N. Siva Shanmugam, and S. Naveenkumar. "Effect of arc length correction on weld bead geometry and mechanical properties of AISI 316L weldments by cold metal transfer (CMT) process." *Materials Today: Proceedings* 18 (2019): 3916-3921.

Keshari, Rahul Kumar, and Poshan Lal Sahu. "Mechanical characterization of dissimilar welded joint of SS202 and SS304 by tungsten inert gas welding." *International Journal of Research in Engineering and Innovation* (2019): 245-252

Koli, Yashwant, N. Yuvaraj, and S. Aravindan. "Investigations on weld bead geometry and microstructure in CMT, MIG pulse synergic and MIG welding of AA6061-T6." *Materials Research Express* 6, no. 12 (2020): 1265e5.

Koli, Yashwant, N. Yuvaraj, and S. Aravindan. "Multi-response Mathematical Modeling for Prediction of Weld Bead Geometry of AA6061-T6 Using Response Surface Methodology." *Transactions of the Indian Institute of Metals* (2020): 1-22.

Kujanpää, Veli. "Thick-section laser and hybrid welding of austenitic stainless steels." *Physics Procedia* 56 (2014): 630-636.

Kumar, A. N. "Modelling of fracture process in annealed sheet of AISI 202 stainless steel." *Modelling Of Fracture Process* 4(3), (1996).

Kumar, N. Pavan, T. Chinnadurai, S. Arungalai Vendan, and N. Sivashanmugam. "Techno economical evaluation for energy analysis in AA6061 during cold metal transfer welding." *Materials Today: Proceedings* 5, no. 11 (2018): 23375-23383.

Kumar, Nalajam Pavan, S. Arungalai Vendan, and N. Siva Shanmugam. "Investigations on the parametric effects of cold metal transfer process on the microstructural aspects in AA6061." *Journal of Alloys and Compounds* 658 (2016): 255-264.

Kumar, S., C. S. Wu, G. K. Padhy, and W. Ding. "Application of ultrasonic vibrations in welding and metal processing: a status review." *Journal of Manufacturing Processes* 26 (2017): 295-322.

KURŞUN, Turhan. "Cold metal transfer (CMT) welding technology." *The Online Journal of Science and Technology-January* 8, no. 1 (2018).

Lei, HaiYang, YongBing Li, and Blair E. Carlson. "Cold metal transfer spot welding of 1 mm thick AA6061-T6." *Journal of Manufacturing Processes* 28 (2017): 209-219.

Lei, Zhenglong, Bingwei Li, Jiang Bi, Pingguo Zhu, Wei Lu, and Jingtao Liu. "Influence of the laser thermal effect on the droplet transfer behavior in laser-CMT welding." *Optics & Laser Technology* 120 (2019): 105728.

Li, Geng, Chen Zhang, Ming Gao, and Xiaoyan Zeng. "Role of arc mode in laser-metal active gas arc hybrid welding of mild steel." *Materials & Design* 61 (2014): 239-250.

Liao, M. T., and W. J. Chen. "The effect of shielding-gas compositions on the microstructure and mechanical properties of stainless steel weldments." *Materials chemistry and physics* 55, no. 2 (1998): 145-151.

Lin, Jian, Ninshu Ma, Yongping Lei, and Hidekazu Murakawa. "Shear strength of CMT brazed lap joints between aluminum and zinc-coated steel." *Journal of materials processing technology* 213, no. 8 (2013): 1303-1310.

Luchtenberg, Paola, Paulo Tancredo de Campos, Paulo Soares, Carlos Augusto Henning Laurindo, Ossimar Maranho, and Ricardo Diego Torres. "Effect of welding energy on the corrosion and tribological properties of duplex stainless steel weld overlay deposited by GMAW/CMT process." *Surface and Coatings Technology* 375 (2019): 688-693.

Lyon, K. N., T. J. Marrow, and S. B. Lyon. "Influence of milling on the development of stress corrosion cracks in austenitic stainless steel." *Journal of Materials Processing Technology* 218 (2015): 32-37.

Mezrag, B., F. Deschaux-Beaume, L. Sabatier, B. Wattrisse, and M. Benachour. "Microstructure and properties of steel-aluminum Cold Metal Transfer joints." *Journal of Materials Processing Technology* 277 (2020): 116414.

Milani, Ali Mehrani, Moslem Paidar, Alireza Khodabandeh, and Saeed Nategh. "Influence of filler wire and wire feed speed on metallurgical and mechanical properties of MIG welding–brazing of automotive galvanized steel/5754 aluminum alloy in a lap joint configuration." *The International Journal of Advanced Manufacturing Technology* 82, no. 9-12 (2016): 1495-1506.

Min, Dong, Jun Shen, Shiqiang Lai, and Jie Chen. "Effect of heat input on the microstructure and mechanical properties of tungsten inert gas arc butt-welded AZ61 magnesium alloy plates." *Materials Characterization* 60, no. 12 (2009): 1583-1590.

Mou, Gang, Xueming Hua, Dongsheng Wu, Ye Huang, Wenhu Lin, and Peizhi Xu. "Microstructure and mechanical properties of cold metal transfer welding-brazing of titanium alloy (TC4) to stainless steel (304L) using V-shaped groove joints." *Journal of Materials Processing Technology* 266 (2019): 696-706.

Nathan, S. Ragu, V. Balasubramanian, S. Malarvizhi, and A. G. Rao. "Effect of welding processes on mechanical and microstructural characteristics of high strength low alloy naval grade steel joints." *Defence Technology* 11, no. 3 (2015): 308-317.

Pradhan, Raghuram, K. M. Krishna Prasad, S. D. Asif, and G. Sai Krishna. "Experimental Investigation And Comparative Study Of Mig &Tig Welding On Ss202 And Ss304 Materials." *International Journal of Recent Scientific Research,* (2019).

Ra, S. U. D. H. A. K. A. R. A. N., SIVASAKTHIVEL PS, and EAZHIL KM. "The effect of welding process parameters on pitting corrosion and microstructure of chromium-manganese stainless steel gas tungsten arc welded plates." *Procedia Engineering* 97 (2014): 790-799.

Rahul, S. G., G. Dhivyasri, P. Kavitha, S. Arungalai Vendan, KA Ramesh Kumar, Akhil Garg, and Liang Gao. "Model reference adaptive controller for enhancing depth of penetration and bead width during cold metal transfer joining process." *Robotics and Computer-Integrated Manufacturing* 53 (2018): 122-134.

Rajeev, G. P., M. Kamaraj, and Srinivasa R. Bakshi. "Effect of correction parameters on deposition characteristics in cold metal transfer welding." *Materials and Manufacturing Processes* 34, no. 11 (2019): 1205-1216.

Reisgen, U., K. Willms, J. Schäfer, M. Türker, J. Hegger, M. Classen, M. Feldmann, and M. Kopp. "Investigations on small-scaled welded structures of austenitic stainless steel." *Kov. Mater* 57 (2019): 397-405.

Schierl, A. "The CMT process a revolution in welding technology." *WELDING IN THE WORLD-LONDON*- 49, no. I (2005): 38.

Selvi, S., A. Vishvaksenan, and E. Rajasekar. "Cold metal transfer (CMT) technology-An overview." *Defence technology* 14, no. 1 (2018): 28-44.

Singh, Ashwani Kuldeep. "Dissimilar Steel Alloys Welding Joint Process Parameters Optimization." *Global Research and Development Journal for Engineering*, 4 (6). 2019

Singh, Jaivindra, Kanwer Singh Arora, and Dinesh Kumar Shukla. "Lap weld-brazing of aluminium to steel using novel cold metal transfer process." *Journal of Materials Processing Technology* (2020): 116728.

Sravanthi, S. S., Swati Ghosh Acharyya, and Praveen Chapala. "Effect of GMAW-brazing and Cold Metal Transfer Welding Techniques on the corrosion behaviour of Aluminium-Steel lap joints." *Materials Today: Proceedings* 18 (2019): 2708-2716.

Stanciu, E. M., A. Pascu, and I. Gheorghiu. "CMT Welding of Low Carbon Steel Thin Sheets." In *IOP Conference Series. Materials Science and Engineering (Online)*, vol. 209, no. 1. 2017.

Taghavi, Farshid, Hasan Saghafian, and Yousef HK Kharrazi. "Study on the effect of prolonged mechanical vibration on the grain refinement and density of A356 aluminum alloy." *Materials & Design* 30, no. 5 (2009): 1604-1611.

Takeda, Yuji, Chatcharit Kiattisaksri, Masatoshi Aramaki, Shinji Munetoh, and Osamu Furukimi. "Effects of specimen thickness in tensile tests on elongation and deformation energy for industrially pure iron." *isij international* (2017): ISIJINT-2016.

Tian, Yinbao, Junqi Shen, Shengsun Hu, Zhijiang Wang, and Jian Gou. "Effects of ultrasonic vibration in the CMT process on welded joints of Al alloy." *Journal of Materials Processing Technology* 259 (2018): 282-291.

Varghese, Paulson, E. Vetrivendan, Manmath Kumar Dash, S. Ningshen, M. Kamaraj, and U. Kamachi Mudali. "Weld overlay coating of Inconel 617 M on type 316 L stainless steel by cold metal transfer process." *Surface and Coatings Technology* 357 (2019): 1004-1013.

Vignesh, G., C. Sathiya Narayanan, C. Pandivelan, K. Shanmugapriya, Bhavishya Naik Tejavath, and Lavuri Tirupathi. "Forming, fracture and corrosion behaviour of stainless steel

202 sheet formed by single point incremental forming process." *Materials Research Express* 6, no. 12 (2019): 126540.

Vignesh, S., B. Mohan, T. Muthuramalingam, and S. Karthikeyan. "Evaluation of recast layer thickness of electrical discharge machined AISI 202 stainless steel with various pulse generators." In *Applied Mechanics and Materials*, vol. 766, pp. 518-522. Trans Tech Publications Ltd, 2015.

Wang, J., Q. Sun, J. Ma, and J. Feng. "Microstructure and mechanical properties of underwater wet welded joint of E40 ship plate steel subjected to ultrasonic vibration." *Tran. China Weld. Ins* 39 (2018): 1-5.

Wang, Ze-long, Zhen-tai Zheng, Li-bing Zhao, Yun-feng Lei, and Kun Yang. "Microstructure evolution and nucleation mechanism of Inconel 601H alloy welds by vibration-assisted GTAW." *International Journal of Minerals, Metallurgy, and Materials* 25, no. 7 (2018): 788-799.

Watanabe, Takehiko, Masataka Shiroki, Atsushi Yanagisawa, and Tomohiro Sasaki. "Improvement of mechanical properties of ferritic stainless steel weld metal by ultrasonic vibration." *Journal of Materials Processing Technology* 210, no. 12 (2010): 1646-1651.

Xu, C., G. Sheng, H. Wang, and X. Yuan. "Reinforcement of Mg/Ti joints using ultrasonic assisted tungsten inert gas welding–brazing technology." *Science and Technology of Welding and Joining* 19, no. 8 (2014): 703-707.

Yang, Jin, Anming Hu, Yulong Li, Peilei Zhang, Dulal Chandra Saha, and Zhishui Yu. "Heat input, intermetallic compounds and mechanical properties of Al/steel cold metal transfer joints." *Journal of Materials Processing Technology* 272 (2019): 40-46.

Yang, Shanglu, Jing Zhang, Jin Lian, and Yongpin Lei. "Welding of aluminum alloy to zinc coated steel by cold metal transfer." *Materials & Design* 49 (2013): 602-612.

Yu, Jiyoung, and Seung Mok Cho. "Metal-cored welding wire for minimizing weld porosity of zinc-coated steel." *Journal of Materials Processing Technology* 249 (2017): 350-357.

Yuan, Tao, Sindo Kou, and Zhen Luo. "Grain refining by ultrasonic stirring of the weld pool." *Acta Materialia* 106 (2016): 144-154.

Zeng, Rong-Chang, Wei Ke, Yong-Bo Xu, E. H. Han, and Z. Y. Zhu. "Recent development and application of magnesium alloys." *Acta Metallurgica Sinica* 37, no. 7 (2001): 673-685.

Zhang, H. T., J. C. Feng, and Peng He. "Interfacial phenomena of cold metal transfer (CMT) welding of zinc coated steel and wrought aluminium." *Materials Science and Technology* 24, no. 11 (2008): 1346-1349.

Zhang, H. T., J. C. Feng, Peng He, B. B. Zhang, J. M. Chen, and L. Wang. "The arc characteristics and metal transfer behaviour of cold metal transfer and its use in joining aluminium to zinc-coated steel." *Materials Science and Engineering: A* 499, no. 1-2 (2009): 111-113.

Zhang, Hong-Tao, Ji-Cai Feng, and Le-Liang Hu. "Energy input and metal transfer behavior of CMT welding process [J]." *Materials Science and Technology* 2 (2012).

Zhao, Guancheng, Zhijiang Wang, Shengsun Hu, Shihua Duan, and Youquan Chen. "Effect of ultrasonic vibration of molten pool on microstructure and mechanical properties of Ti-6Al-4V joints prepared via CMT+ P welding." *Journal of Manufacturing Processes* 52 (2020): 193-202.